

High dimensional Single Index Bayesian Modeling of the Brain Atrophy over time

Arkaprava Roy^{*,†}, Subhashis Ghosal^{*,‡} Kingshuk Roy Choudhury[†] and For The Alzheimer's Disease Neuroimaging Initiative[§]

Abstract. We study the effects of gender, APOE genes, age, genetic variation and Alzheimer's disease on the atrophy of the brain regions. In the real data analysis section, we add a subject specific random effect to capture subject inhomogeneity. A nonparametric single index Bayesian model is proposed to study the data with B-spline series prior on the unknown functions and Dirichlet process scale mixture of zero mean normal prior on the distributions of the random effects. Posterior consistency of the proposed model without the random effect is established for a fixed number of regions and time points with increasing sample size. A new Bayesian estimation procedure for high dimensional single index model is introduced in this paper. Performance of the proposed Bayesian method is compared with the corresponding least square estimator in the linear model with LASSO and SCAD penalization on the high dimensional covariates. The proposed Bayesian method is applied on a dataset of 748 individuals with 620,901 SNPs and 6 other covariates for each individual.

Keywords: ADNI, Bayesian, GWAS, High dimensional data, Single Index Model, Spike and Slab prior.

1 Introduction

Alzheimer disease (AD) is a progressive neurodegenerative disease that affects approximately 5.5 million people in the United States and about 30 million people worldwide. It is believed to have a prolonged preclinical phase initially characterized by the development of silent pathologic changes when patients appear to be clinically normal, followed by mild cognitive impairment (MCI) and then dementia (AD) (Petrella (2013)). Apart from its manifestation in the impairment of cognitive abilities, disease progression also produces a number of structural changes in the human brain, which includes the deposition of amyloid protein and the shrinkage or atrophy for certain regions of the brain

^{*}Department of statistics
North Carolina State University
Stinson Dr, Raleigh, NC 27607
aroy2@ncsu.edu sghoshal@ncsu.edu

[†]Dept. of Biostatistics and Bioinformatics,
Duke University Medical Center,
Durham, NC kingshuk.roy.choudhury@duke.edu

[‡]Research is partially supported by NSF grant DMS-1510238.

[§]Data used in preparation of this article were obtained from the Alzheimer's Disease Neuroimaging Initiative (ADNI) database (adni.loni.usc.edu). As such, the investigators within the ADNI contributed to the design and implementation of ADNI and/or provided data but did not participate in analysis or writing of this report. A complete listing of ADNI investigators can be found at: http://adni.loni.usc.edu/wp-content/uploads/how_to_apply/ADNI_Acknowledgement_List.pdf

over time ([Thompson et al. \(2003\)](#)). Previous studies have shown that the rate of brain atrophy is significantly modulated by a number of factors, such as gender, age, baseline cognitive status and most markedly, allelic variants in the APOE gene ([Hostage et al. \(2014\)](#)). In this paper, we examine if any other genes are also implicated in modulating the rate of brain atrophy. This analysis represents a technical challenge because the genomic data is high dimensional and needs to be incorporated in a model for longitudinal progression of brain volumes measured in multiple parts of the brain.

Our study uses the data collected by Alzheimer's Disease Neuroimaging Initiative (ADNI). In this dataset, volumes of thirteen disjoint brain regions are recorded over six visits after every six months. With age these volumes change and Alzheimer's disease makes these changes much more pronounced. Genetic variations also have impacts on the configuration of the brain. Factors such as gender, age etc. are also responsible for these changes. In this paper, we propose a model for the volume of different brain regions to quantify the effects of different factors on the volume of brain regions. The regions, we studied here, are depicted in the Figure 1. This image is obtained from [Ahveninen et al. \(2012\)](#).

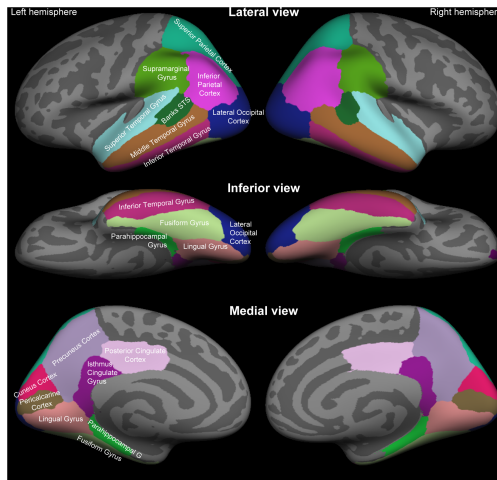


Figure 1: Anatomic parcellation of cortical surface from different angles

We consider volumetric measurements of thirteen disjoint brain regions that are recorded over time along with that for volume of the grey matter. At a given time point, the volume of a particular region will depend on the initial configuration and rate of change of that region. We consider two sets of unknown functions of covariates to model these initial configurations and rates of changes for different regions with two inputs, one from a high dimensional SNP and another from a low-dimensional vector other covariates. These functions will look like $\{(a_{0,j}(X'\beta, Z\eta)\}$ for the initial configuration and $\{a_{1,j}(X'\beta, Z\eta)\}_{1 \leq j \leq 14}\}$ for the rate of change in j -th region; here X and Z are high and low dimensional covariates respectively. These functions are modeled by a bivariate single index model and a finite random series prior is put on the function based on

tensor products of B-splines with appropriate prior distribution on the coefficients. We reparametrize the coefficients of the covariates in the single index to ease the estimation of this model. After the reparametrization, due to high dimensionality of the SNP data we carefully put prior for a desired shrinkage in the estimate. To incorporate the effect of time for analyzing our dataset, we consider an increasing function of time into the model. This is also estimated nonparametrically with a finite random series prior on the function based on B-spline with appropriate prior on the coefficients.

Apart from modeling volume of brain regions over time in terms of SNP and external covariates and obtaining Bayes estimates, the proposed method develops an estimation scheme for a general high dimensional single index model. Estimation for high dimensional single index model is addressed in [Zhu and Zhu \(2009\)](#), [Yu and Ruppert \(2002\)](#), [Wang et al. \(2012\)](#), [Peng and Huang \(2011\)](#), [Radchenko \(2015\)](#) and [Luo and Ghosal \(2016\)](#). All of them used l_1 penalty and worked out an optimization technique to get the estimates. In Bayesian framework, [Antoniadis et al. \(2004\)](#) used Fisher–von Mises prior on the directional vector. This can not be easily modified for high dimensional case as then we need a prior which favors larger number of zeros in the unit vector. That will make the prior too complex to use. Another paper addressing sparse Bayesian single index model estimation is [Alquier and Biau \(2013\)](#). Even though their method is theoretically attractive, due to high computational complexity it is difficult to implement when the number of covariates is very high. In [Wang \(2009\)](#), they developed a sparse Bayesian estimation for sparse single index model using reversible jump Markov chain Monte Carlo technique which puts a lot of computational burden in estimating the model parameters. These methods are extremely difficult to implement for extreme high dimensional cases. For affordable computation using our method, we provide an R package for estimation in single index model with inputs both in high and low dimensional setup.

The rest of the paper is arranged in the following manner. The next section discusses the dataset and modeling in more detail. In Section 3, we describe the prior on different parameters of the model. Section 4 describes posterior computation in this setup. We provide a simulation study comparing the proposed Bayesian procedure with its linear counterpart in Section 5. We study posterior consistency in the model in Section 6 under the asymptotic regime where the number of individuals goes to infinity but the number of time points where measurements are taken and the number of regions are fixed. The posterior consistency result justifies the use of the proposed Bayesian procedure from a frequentist perspective. In Section 7 we present the results from a real data analysis. Section 8 concludes the paper with some further remarks.

2 Data description and modeling

Data used in the preparation of this article were obtained from the Alzheimer’s Disease Neuroimaging Initiative (ADNI) database ([adni.loni.usc.edu](#)). ADNI was launched in 2003 as a public-private partnership, led by Principal Investigator Michael W. Weiner, MD. The primary goal of ADNI has been to test whether serial magnetic resonance imaging (MRI), positron emission tomography (PET), other biological markers, and

clinical and neuropsychological assessment can be combined to predict the progression of mild cognitive impairment (MCI) and early Alzheimer's disease (AD). In the ADNI dataset, the grey matter part of the brain is divided into thirteen disjoint regions. The volume of these regions and the whole brain are recorded over time for $n = 748$ individuals. The number of visits is not uniform across individuals, but varies between 1 to 6. The volume data of $J = 14$ components of brain over T_i many time points for the i -th individual, for $i = 1, \dots, 748$ is collected where $1 \leq T_i \leq 6$.

Apart from the volumetric measurements, we also have high dimensional SNP data and data on some other covariates for each individual. The other covariates are gender, disease state, age and allele 2 and 4 of APOE gene. Except for the covariate age, all other low-dimensional covariates are categorical. To represent categorical variables, we use binary dummy variables. Since the disease status has three states : NC (no cognitive impairment), MCI (mild cognitive impairment) and AD (Alzheimer's disease). We consider two dummy variable Z^{AD} and Z^{MCI} respectively standing for the onset of MCI and AD, setting NC at the baseline. Similarly the dummy variable Z^M indicating male gender is introduced setting females at the baseline. Also we introduce $Z^{APOE,3}$, $Z^{APOE,4}$ standing for alleles 2 and 4 for the two alleles APOEallele2 and APOEallele4 together setting allele 3 as baseline for each of the two cases. Let $Z = (Z^{MCI}, Z^{AD}, Z^M, \text{Age}, Z^{APOE,3}, Z^{APOE,4})$ stand for the whole vector of covariates. The continuous variable, Age, is standardized. Along with that, we have SNP data for each individual. In ADNI, the subjects were genotyped using participants the Human 610-Quad BeadChip (Illumina, Inc., San Diego, CA) was used. We have a set of 620,901 SNP and copy number variation (CNV) markers. The APOE gene has been the most significant gene in GWAS of Alzheimer's disease. The corresponding SNPs, rs429358 and rs7412, are not on the Human 610-Quad Bead-Chip. At the time of participant enrollment APOE genotyping was performed and included in the ADNI database. The two SNPs (rs429358, rs7412) define the epsilon 2, 3, and 4 alleles and therefore were genotyped using DNA extracted by Cogenics from a 3 mL aliquot of EDTA blood. These alleles are considered separately in the study.

With time, different brain regions change differently. We study the effects of different attributes to these changes. For every individual, the volume of a brain region on a particular visit should primarily depend on the volume of that region at the zeroth visit and the rate of change of volume for that region with time. These components are not uniform across individuals or regions. Hence, it will be logical to consider that the baseline volume, recorded at the initial visit and the rate of change as a function of the region and the individual covariates. As the geometry of brain structure is complicated, we don't assume a form of standard spatial dependence between measurements across brain regions. Thus we need two sets $\{(a_{0,j}(\cdot), a_{1,j}(\cdot))_{1 \leq j \leq 14}\}$ of functions for modeling volume at the initial visit and the rate of change for the j -th region. These functions are unknown and are modeled nonparametrically. For nonparametric regression problems, single-index models provide a lot of flexibility in estimation and interpretation of the results. Hence, we adopt the bivariate single-index model with two inputs for high-dimensional and low-dimensional covariates separately for easy interpretation and computational efficiency. The effect of time is captured through an unknown increasing function $F_0(\cdot)$, which is bounded in $[0, 1]$. This is also modeled nonparametrically.

Thus the data generating process can be represented through the following specification

$$\begin{aligned} Y_{ijt} &= F(i, j, t) + \epsilon_{ijt}, \epsilon_{ijt} \sim \mathbb{N}(0, \sigma^2), \\ F(i, j, t) &= a_{0,j}(X_i' \beta, Z_i' \eta) - a_{1,j}(X_i' \beta, Z_i' \eta) F_0(t), \end{aligned} \quad (2.1)$$

where Y_{ijt} is the volume of the j -th brain region for the i -th individual at the t -th time point in logarithmic scale, X_i is high-dimensional SNP expression of length p for the i -th individual and $a_{0,j}(\cdot), a_{1,j}(\cdot), F_0(\cdot)$ are all unknown functions satisfying the condition that F_0 is continuous, monotone increasing function form $[0, 1]$ onto $[0, 1]$. For identifiability of the functions along with the parameters β and η , we assume that $\|\beta\|_2 = 1$, $\|\eta\|_2 = 1$ and that the first non zero coefficients of β and η are positive; here $\|\cdot\|_2$ denotes L_2 -norm of a vector. The biggest challenge for estimation in this model is the high dimensionality of β . We normalize the covariates for each individual i.e. X_i and $Z_{t,i}$ for each combination of (t, i) such that the norm is one. This is to make the inputs of the functions bounded between $[-1, 1]$. We view Z_i as an abstract covariate of dimension k . Due to the high dimensionality of β , we propose a sparse estimation scheme. First we reparametrize the two unit vector $\beta = (\beta_1, \dots, \beta_p)$ and $\eta = (\eta_1, \dots, \eta_k)$ to their respective polar forms which allows us to work with Euclidean spaces. In the polar setup, for $s \leq p-1$, $\beta_s = \prod_{l=1}^{s-1} \sin \theta_l \cos \theta_s$, and $\beta_p = \prod_{l=1}^{p-1} \sin \theta_l$ where $\{\theta = (\theta_1, \dots, \theta_{p-1})\}$ is the polar angle corresponding to the unit vector β . Here $\theta_s \in [0, \pi]$ for $s \neq (p-1)$ and $\theta_{p-1} \in [0, 2\pi]$. Similarly, let α be the polar angle corresponding to η . Then for $s \leq k-1$, $\eta_s = \prod_{l=1}^{s-1} \sin \alpha_l \cos \alpha_s$ and $\eta_k = \prod_{l=1}^{k-1} \sin \alpha_l$.

3 Prior specification

In the nonparametric Bayesian setup described above, we induce prior distributions on the smooth functions a_0^j and a_1^j in (2.1) through basis expansions in tensor products of B-splines and prior on the corresponding coefficients. Given other parameters in this setup, a normal prior distribution on the coefficients of the tensor products of B-splines will lead to conjugacy and faster sampling via Gibbs sampling scheme. An inverse gamma prior on σ^2 is an obvious choice due to conjugacy and faster sampling. We also put a B-spline series prior on the smooth increasing function of time $F_0(\cdot)$. The coefficients for this function would be increasing in the index of the basis functions and lie in $(0, 1]$. To put prior on an increasing sequence, we introduce a set of latent variables of size equal to number B-spline coefficients. Then the B-spline coefficients would be normalized cumulative sum of those latent variables. Other two parameters β and η are reparametrized into their polar co-ordinate system. The parameter space of the polar angles will be a hyperrectangle. It will be easier to put prior on polar angles. To estimate using the sparsity of β , we need to carefully put a shrinkage prior on the polar angles. A polar angle of $\pi/2$ will ensure that the corresponding co-ordinate in the unit vector equal to zero. When there is sparsity in the unit vector, most of polar angles will become $\pi/2$. Thus a spike and slab prior on polar angle with spike at $\pi/2$ should be able to capture sparsity in the corresponding unit vector. Last polar angle can either be 0 or $\pi/2$, depending on last or penultimate co-ordinate of the unit should be zero.

The priors are described in detail below:

(i) Intercept and slope functions:

$$a_0(x, y) = \sum_{m=1}^K \sum_{m'=1}^K \lambda_{0,mm'}^j B_m(x) B_m'(y),$$

$$a_1(x, y) = \sum_{m=1}^K \sum_{m'=1}^K \lambda_{1,mm'}^j B_m(x) B_m'(y),$$

– the function coefficients: For some chosen $a > 0$,

$$\lambda_{t,mm'}^j \sim N(0, a^2), \quad \lambda_{1,mm'}^j \sim N(0, a^2), \quad 1 \leq m, m' \leq K.$$

(ii) The function of time:

$$F_0(x) = \sum_{m=1}^K \lambda_m B_m(x),$$

– For the above function we need $\lambda_1 = 0$ and $\lambda_K = 1$. For estimation of the coefficients we introduce a new set of latent variables $(\delta_1, \dots, \delta_{K-1})$

$$\delta_i \sim Un(0, 1), \quad \lambda_{m+1} = \frac{\sum_{i=1}^m \delta_i}{\sum_{i=1}^{K-1} \delta_i}$$

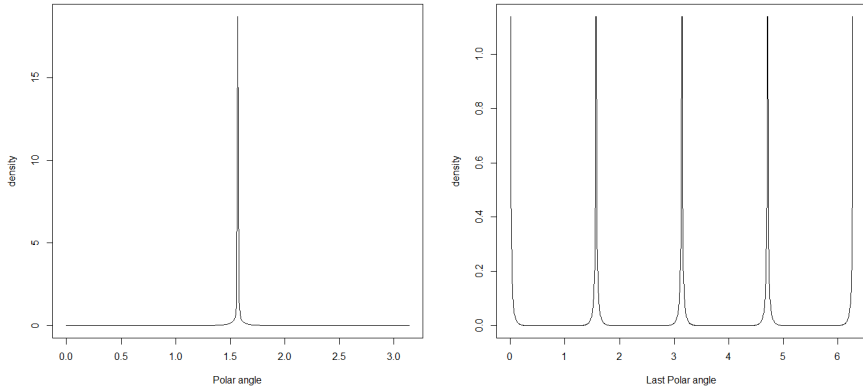
for $m = 1, \dots, K-1$ and here Un stands for the uniform distribution. This approach to model increasing co-efficients was earlier used by [Das and Ghosal \(2017\)](#).

(iii) Error variance: $\sigma^{-2} \sim Ga(d_1, d_2)$, where Ga stands for the gamma distribution.

(iv) Polar angles α of η : We put independent $Un(0, \pi)$ prior on α_i for $i = 1, \dots, (k-2)$ and $\alpha_{k-1} \sim Un(0, 2\pi)$

(v) Polar angles θ of β : We reparametrize the polar angles as $\theta'_i = 1 - \frac{\min(\theta_i, \pi - \theta_i)}{\pi/2}$ for $1 \leq i \leq (p-2)$. And $\theta''_{p-1} = \frac{\theta_{p-1}}{\pi/2} - \mathbb{1}(\theta_{p-1} > \pi/2) - \mathbb{1}(\theta_{p-1} > \pi) - \mathbb{1}(\theta_{p-1} > 3\pi/2)$. Then we would reduce it further to $\theta'_{p-1} = \frac{4}{\pi} \min(\theta''_{p-1}, \pi/2 - \theta''_{p-1})$. Then we put a spike and slab prior $\theta'_i \sim (1 - \gamma)Be(M_1, M_2) + \gamma Un(0, 1)$, where Be stands for the Beta distribution.

To incorporate for first non-zero coefficient to be positive, the support for the polar angles upto the first non-zero coefficient in β or η is set to $[0, \pi/2]$. The spike distribution on θ looks like Figure 2. The first plot is for the first $p-2$ angles and the second plot is for the last polar angle.

Figure 2: Spike distribution with $M_1 = 0.01$ and $M_2 = 10$.

4 Computation

Introduce a latent variable I_l for the indicator of the $\text{Un}(0,1)$ component of the distribution of θ'_l , $l = 1, \dots, p-1$. Now the log-likelihood is given by

$$\begin{aligned}
C - \sum_{i,j,t} \frac{1}{2\sigma^2} & \left(Y_{ijt} - \sum_{m=1}^K \sum_{m'=1}^K \lambda_{0,mm'}^j B_m \left(\sum_{s=1}^{p-1} X_{is} \prod_{l=1}^{s-1} \sin \theta_l \cos \theta_s \right. \right. \\
& \left. \left. + X_{ip} \prod_{l=1}^{p-1} \sin \theta_l \right) B'_m \left(\sum_{s=1}^{k-1} Z_{is} \prod_{l=1}^{s-1} \sin \alpha_l \cos \alpha_s + Z_{ik} \prod_{l=1}^{k-1} \sin \alpha_l \right) \right. \\
& \left. + \sum_{m=1}^K \sum_{m'=1}^K \lambda_{1,mm'}^j B_m \left(\sum_{s=1}^{p-1} X_{is} \prod_{l=1}^{s-1} \sin \theta_l \cos \theta_s + X_{ip} \prod_{l=1}^{p-1} \sin \theta_l \right) B'_m \left(\sum_{s=1}^{k-1} Z_{is} \prod_{l=1}^{s-1} \sin \alpha_l \cos \alpha_s \right. \right. \\
& \left. \left. + Z_{ik} \prod_{l=1}^{k-1} \sin \alpha_l \right) \sum_{m=1}^{K-1} \frac{\sum_{i=1}^m \delta_i}{\sum_{i=1}^{K-1} \delta_i} B_{m+1}(t) \right)^2 - \sum_{m,n,j} \frac{(\lambda_{0,mn}^j)^2 + (\lambda_{1,mn}^j)^2}{2a^2} \\
& + \sum_{l=1}^{p-1} \log((1 - I_l) \theta_l^{M_1-1} (1 - \theta'_l)^{M_2-1} \frac{\Gamma(M_1 + M_2)}{\Gamma(M_1)\Gamma(M_2)} + I_l) + I_l \log \gamma \\
& + (1 - I_l) \log(1 - \gamma) - (J \sum_i T_i/2 + d_1 - 1) \log \sigma^2 - d_2/\sigma^2,
\end{aligned}$$

where C involves only the hyperparameters a, M_2, M_1, K, d_1, d_2 and the observations but not parameter of the model.

All the B-spline coefficients and σ are updated using the conjugacy structure.

Posterior updates are described here. For notational convenience, we define $\lambda_0^j = \{\lambda_{0,mm'}^j : 1 \leq m, m' \leq K\}$, $\lambda_1^j = \{\lambda_{1,mm'}^j : 1 \leq m, m' \leq K\}$, $\delta = (\delta_1, \dots, \delta_{K-1})$, $\theta = \{\theta_i : 1 \leq i \leq (p-1)\}$ and $\alpha = \{\alpha_i : 1 \leq i \leq (k-1)\}$, $X_i' \beta = \sum_{s=1}^{p-1} X_{is} \prod_{l=1}^{s-1} \sin(\theta_l) \cos(\theta_s) + X_{ip} \prod_{l=1}^{p-1} \sin(\theta_l)$, $Z_i' \eta = \sum_{s=1}^{k-1} Z_{is} \prod_{l=1}^{s-1} \sin(\alpha_l) \cos(\alpha_s) + Z_{ik} \prod_{l=1}^{k-1} \sin(\alpha_l)$, $\psi_i = \{B_m(X_i' \beta) B_{m'}(Z_i' \eta) : 1 \leq m, m' \leq K\}$. Below we use Id_l to denote identity matrix of dimension l .

- Updating σ : Posterior density of σ is inverse gamma with parameters d_1, d_2 .
- Updating λ_0^j : The posterior variance ($V_{0,j}$) and posterior mean ($M_{0,j}$) are respectively $V_{0,j} = 2(\sigma^{-2} \sum_i T_i \psi_i \psi_i' + a^{-2} \text{Id}_{K^2})^{-1}$ and $M_{0,j} = V_{0,j} [\sum_i \psi_i \sum_{t=0}^{T_i} (Y_{ijt} + \sum_{m=1}^K \sum_{m'=1}^K \lambda_{1,mm'}^j B_m(X_i' \beta) B_{m'}(Z_i' \eta) \frac{1}{\sum_{i=1}^{K-1} \delta_i} \sum_{m=1}^{K-1} \sum_{i=1}^m \delta_i B_{m+1}(t))]$
- Updating λ_1^j : The posterior variance ($V_{1,j}$) and posterior mean ($M_{1,j}$) are respectively $V_{1,j} = 2(\sigma^{-2} \sum_i \psi_i \psi_i' (\sum_{t=1}^{T_i} \frac{1}{\sum_{i=1}^{K-1} \delta_i} \sum_{m=1}^m \delta_i B_{m+1}(t))^2 + \text{Id}_{K^2}/a^2)^{-1}$ and $M_{1,j} = V_{1,j} [\sum_i \psi_i \sum_{t=0}^{T_i} (Y_{ijt} - \sum_{m=1}^K \sum_{m'=1}^K \lambda_{0,mm'}^j B_m(X_i' \beta) B_{m'}(Z_i' \eta)) \frac{1}{\sum_{i=1}^{K-1} \delta_i} \sum_{m=1}^{K-1} \sum_{i=1}^m \delta_i B_{m+1}(t)]$.
- Updating θ_i : Sample by the Metropolis-Hastings algorithm
 - Generate U_{1i} from $\text{Be}(B_1, B_1)$;
 - Update θ_i to $\theta_i^* = \begin{cases} \frac{\pi \frac{\theta_i U_{1i}}{\theta_i U_{1j} + (\pi - \theta_i)(1 - U_{1i})}}{2\pi \frac{\theta_i U_{1i}}{\theta_i U_{1j} + (2\pi - \theta_i)(1 - U_{1i})}}, & \text{if } i < p-1, \\ \frac{\theta_i U_{1i}}{\theta_i U_{1j} + (2\pi - \theta_i)(1 - U_{1i})}, & \text{if } i = p-1. \end{cases}$

Conditional density of this update is given by

$$f(\theta_i^* | \theta_i) = \frac{\left(\frac{\theta_i'(1-\theta_i'^*)}{\theta_i' + \theta_i'^* - 2\theta_i'\theta_i'^*}\right)^{B_1-1} \left(1 - \frac{\theta_i'(1-\theta_i'^*)}{\theta_i' + \theta_i'^* - 2\theta_i'\theta_i'^*}\right)^{B_1-1}}{B(B_1, B_1)} \frac{\theta_i'^*(1 - \theta_i'^*)}{(\theta_i' + \theta_i'^* - 2\theta_i'\theta_i'^*)^2}$$

where θ_i' is as in item (v) of the prior specification part.

The acceptance probability in Metropolis-Hastings algorithm is then given by

$$P_{a,\theta_i} = \min \left\{ \frac{L_1(i, \theta_i^*) f(\theta_i | \theta_i^*)}{L_1(i, \theta_i) f(\theta_i^* | \theta_i)}, 1 \right\};$$

here $L_1(i, x)$ denotes the likelihood for $\theta_i = x$. We need to tune B_1 to achieve a good acceptance rate. This approach is due to [Roy et al. \(2017\)](#).

- Updating α_i : Sampling by the Metropolis-Hastings algorithm
 - Generate U_{2i} from $\text{Be}(B_2, B_2)$

- Update α_i to $\alpha_i^* = \begin{cases} \pi \frac{\alpha_i U_{2i}}{\alpha_i U_{2j} + (\pi - \alpha_i)(1 - U_{2i})}, & \text{if } i < k - 1, \\ 2\pi \frac{\alpha_i U_{2i}}{\alpha_i U_{2j} + (2\pi - \alpha_i)(1 - U_{2i})}, & \text{if } i = k - 1. \end{cases}$

The conditional density of this update is given by

$$f_1(\alpha_i^* | \alpha_i) = \frac{\left(\frac{\zeta_i(1-\zeta_i^*)}{\zeta_i + \zeta_i^* - 2\zeta_i\zeta_i^*}\right)^{B_2-1} (1 - \frac{\zeta_i(1-\zeta_i^*)}{\zeta_i + \zeta_i^* - 2\zeta_i\zeta_i^*})^{B_2-1}}{B(B_2, B_2)} \frac{\zeta_i^*(1 - \zeta_i^*)}{(\zeta_i + \zeta_i^* - 2\zeta_i\zeta_i^*)^2},$$

where $\zeta_i = \alpha_i/\pi$, $\zeta_i^* = \alpha_i^*/\pi$ for $i < k - 1$ and $\zeta_{k-1} = \alpha_{k-1}/2\pi$, $\zeta_{k-1}^* = \alpha_{k-1}^*/2\pi$

The acceptance probability in the Metropolis-Hastings algorithm is then given by

$$P_{a,\alpha_i} = \min\left\{\frac{L_2(i, \alpha_i^*) f_1(\alpha_i^* | \alpha_i)}{L_2(i, \alpha_i) f_1(\alpha_i^* | \alpha_i)}, 1\right\};$$

here $L_2(i, x)$ denotes the likelihood for $\alpha_i = x$. We need to tune B_2 to achieve a good acceptance rate.

- Updating δ : Sampling by the block Metropolis-Hastings algorithm :

- Generate from U_3 of length $K - 1$, each from $\text{Be}(B_3, B_3)$;
- Update δ_j to $\delta_j^* = \frac{\delta_j U_{3j}}{\delta_j U_{3j} + (1 - \delta_j)(1 - U_{3j})}$.

Elementary calculations give us the conditional density of this update as

$$f(\delta^* | \delta) = \prod_{j=1}^{K-1} \frac{\left(\frac{\delta_j(1-\delta_j^*)}{\delta_j + \delta_j^* - 2\delta_j\delta_j^*}\right)^{B_3-1} (1 - \frac{\delta_j(1-\delta_j^*)}{\delta_j + \delta_j^* - 2\delta_j\delta_j^*})^{B_3-1}}{B(B_3, B_3)} \frac{\delta_j^*(1 - \delta_j^*)}{(\delta_j + \delta_j^* - 2\delta_j\delta_j^*)^2}$$

The acceptance probability in Metropolis-Hastings algorithm is then given by

$$P_{a,\delta_j} = \min\left\{\frac{L_3(\delta^*) f(\delta^* | \delta)}{L_3(\delta) f(\delta^* | \delta)}, 1\right\};$$

here $L_3(x)$ denotes the likelihood for $\delta = x$. We need to tune B_3 to achieve a good acceptance rate.

Due to the large size of the vector θ , one can consider updating in chunks. For ultra-high dimension, we update θ in chunks of size 30 coordinates. From each post burn-in sample we get the angles, that should be included in the model according to the latent indicator variable I . Default value of each polar angle is considered to be $\pi/2$. This way if an angle is not in the model, in the rectangular system, the corresponding co-ordinate will be zero.

5 Simulation

We compare our model with following simplified linear model :

$$\log(Y_{ijt}) = X'_i \beta + Z'_i \eta + \gamma_{1,j} - (X'_i \beta + Z'_i \eta + \gamma_{2,j})t + e_{ijt} \quad (5.1)$$

In the above model, β is a sparse vector and all other parameters are unpenalized. The performance of these two models are compared based on MSE values on test set. For sample sizes 200, 500 and 1000, we gather the MSE values corresponding to those models both for well-specified and misspecified cases. We use half of the sample for training and the remaining half for testing. Among other parameters we consider 13 regions in total, 5 time points and vary the value of p as 5000, 10000 and 20000. We include one case for ultra high dimension of $p = 100000$ and sample size 200. We set $M_1 = 0.1$ and tune M_2 for different cases to ensure a good acceptance rate and desired model size (sum of q_i 's) across MCMC samples. The results are summarized below for 30 replications and 1000 post burn-in samples. The number of basis functions for spline is different across different sample sizes. For the ultra-high dimensional case with $p = 100000$ and $n = 200$, we consider 10 replications.

Data generation for the non-linear case:

- Generate a data matrix X with elements coming from Bernoulli distribution with success probability of i^{th} row as p_i .
- Generate p_i 's from the standard uniform distribution.
- Generate all the elements of the matrix Z from $N(0, 1)$.
- Generate the sparse vector β with 5% elements non-zero. Positions for non-zero elements are chosen first at random by sampling $p/20$ elements from total p positions. Here p is the length of β . The non zero elements are generated from mixture distribution of two normals $N(2, 1)$ and $N(-1, 1)$.
- Set the value of η to $(1, -2, 4.3, 10, -8)$.
- Construct the intercept and slopes from functions through tensor products of B-splines with 11 basis functions in each direction, the coefficients for the intercept functions from $N(2, 1)$ and for slopes from $N(-1, 1)$.
- Normalize each row of X and Z along with β are η to the unit norm.

After generating the design matrix, the data Y_{ijt} is generated from $N(a_{0,j}(X'_i \beta, Z'_i \eta) - a_{1,j}(X'_i \beta, Z'_i \eta)F_0(t), 1)$.

Data generation for the linear case:

In this case, the true model is the one given in (5.1). All the steps for generating X , Z , β and η are similar as above. The coefficients $\gamma_{1,j}$'s and $\gamma_{2,j}$'s are generated from $N(0, 1)$. After generating the design matrix, the data Y_{ijt} is generated from $N(X_i \beta + Z_i \eta + \gamma_{1,j} - (X_i \beta + Z_i \eta + \gamma_{2,j})t, 1)$

For data generation, we set the error standard deviation $\sigma_0 = 1$.

We split the whole data into two equal parts for training and testing. We compare the performance of our method with LASSO (Tibshirani (1996)) and SCAD (Fan and Li (2001)) on testing dataset based estimates of parameters from training dataset. We use the R package `glmnet` for LASSO and `ncvreg` for SCAD. To fit our model we vary the the number of B-spline basis function as 8 for 200 case, 11 for 500 case, and 14 for 1000 case. These values are considered based on asymptotic rate of contraction of number of B-spline basis functions.

Table 1: For non-linear case

Total sample size	Dimension of β (p)	SIM	LASSO	SCAD
		MSE	MSE	MSE
200	5000	1.28	8.92	1.45
200	10000	1.43	8.86	1.50
200	20000	1.45	9.03	1.61
500	5000	1.14	7.22	1.41
500	10000	1.19	7.82	1.46
500	20000	1.33	8.44	1.50
1000	5000	1.01	6.28	1.41
1000	10000	1.07	6.7	1.45
1000	20000	1.15	7.33	1.50
200	100000	1.14	7.32	1.43

Table 2: For linear case

Total sample size	Dimension of β (p)	SIM	LASSO	SCAD
		MSE	MSE	MSE
200	5000	1.36	1.04	1.10
200	10000	1.50	1.07	1.07
200	20000	1.67	1.12	1.03
500	5000	1.31	1.03	1.07
500	10000	1.47	1.04	1.07
500	20000	1.61	1.04	1.06
1000	5000	1.26	1.02	1.08
1000	10000	1.37	1.04	1.06
1000	20000	1.61	1.04	1.04
200	100000	1.12	1.02	1.05

From the Table 1 and 2, we infer that the performance of our Bayesian method based on the high dimensional single index model is always better than the LASSO and the SCAD for non-linear case. For linear case, it is competitive with linearity based methods like the LASSO or the SCAD. This is natural as the LASSO or the SCAD use more precise modeling information which on semiparametric methods cannot compete on.

6 Large-sample Properties

We examine large sample properties of the proposed Bayesian procedure for the model in this section. We have observations for fixed J number of regions and T many time points. We show posterior consistency in the asymptotic regime of increasing sample size and increasing dimension (p) of SNPs. We need to establish some preliminary results before getting into the consistency results. The first result relates the Euclidean distance between two unit vectors with the corresponding polar angles.

Lemma 1. *Let β_1 and β_2 are two unit vectors and θ_1 and θ_2 are their corresponding polar co-ordinates. Then $\|\beta_1 - \beta_2\|_2^2 \leq 4\|\theta_1 - \theta_2\|_2^2$*

The proof is given in the Section 10.

We have the following set up in the model:

$$Y_{ijt} = F(i, j, t) + \epsilon_{ijt}, \quad \epsilon_{ijt} \sim N(0, \sigma^2),$$

$$F(i, j, t) = a_0^j(X_i' \beta, Z_i' \eta) - a_1^j(X_i' \beta, Z_i' \eta) F_0(t).$$

Here $i = 1, \dots, N$, $j = 1, \dots, J$ and $t = 1, \dots, T_i$. Let Π denote a probability measure on \mathcal{P} , as a subset of all probability measures. For $P, Q \in \mathcal{P}$, let

$$K(p, q) = P \log \frac{p}{q} \quad V(p, q) = P \log^2 \frac{p}{q}$$

We also use Hellinger distance $d_H(P, Q) = \sqrt{\int (\sqrt{p} - \sqrt{q})^2}$.

Let P_{0i} denote the true distribution with density p_{0i} for i -th individual. For each individual i , we consider the observation Y_i of length $J \times T_i$ and $Y_i \sim \text{MVN}(\mu_i, \sigma^2 I_{J \times T_i})$; here $\mu_i = \{F(i, j, t) : j = 1, \dots, J \text{ and } t = 1, \dots, T_i\}$

For $p_i = \text{MVN}(\mu_1^i, \sigma_1^2 I_k)$ and $q_i = \text{MVN}(\mu_2^i, \sigma_2^2 I_k)$, we have

$$K(p_i, q_i) = k \log \left(\frac{\sigma_2}{\sigma_1} \right) - \frac{1}{2} \left[k - \frac{(\mu_1^i - \mu_2^i)'(\mu_1^i - \mu_2^i)}{\sigma_2^2} - k \frac{\sigma_1^2}{\sigma_2^2} \right]$$

$$V(p_i, q_i) = \frac{k}{2} \left(\frac{\sigma_1^2}{\sigma_2^2} - 1 \right)^2 + k \frac{(\mu_1^i - \mu_2^i)'(\mu_1^i - \mu_2^i)}{\sigma_2^4} \sigma_1^2$$

$$d_H^2(P, Q) = 1 - \left(\frac{2\sigma_1\sigma_2}{\sigma_1^2 + \sigma_2^2} \right)^{k/2} \exp \left(- \frac{(\mu_1 - \mu_2)'(\mu_1 - \mu_2)}{4(\sigma_1^2 + \sigma_2^2)} \right).$$

Lemma 2. *In the above setup we have $d_H^2(P, Q) \leq \frac{(\sigma_1 - \sigma_2)^2}{(\sigma_1^2 + \sigma_2^2)} + (\mu_1 - \mu_2)'(\mu_1 - \mu_2)$ and for some $C > 2$ and μ_1, μ_2 close enough, $Cd_H^2(P, Q) \geq \frac{(\sigma_1 - \sigma_2)^2}{\sigma_1^2 + \sigma_2^2} + \frac{(\mu_1 - \mu_2)'(\mu_1 - \mu_2)}{2(\sigma_1^2 + \sigma_2^2)}$*

The proof is in the Section 10.

We denote $\Theta = (\beta, \eta, \sigma, a_0, a_1, F_0)$ as set of parameters. Let $\Theta_1 = (\beta_1, \eta_1, \sigma_1, a_{0,1}, a_{1,1}, F_{0,1})$ and $\Theta_2 = (\beta_2, \eta_2, \sigma_2, a_{0,2}, a_{1,2}, F_{0,2})$ be two such sets of parameters. We use $\|\cdot\|_\infty^2$ to denote the supremum norm.

Upper bound for the Hellinger distance

We can show for two functions approximated with D many B-spline basis functions along each direction, $\|a_{0,1}^j - a_{0,2}^j\|_\infty^2 \leq \|\phi_{0,1}^j - \phi_{0,2}^j\|_\infty^2$, where $\phi_{0,1}^j$ and $\phi_{0,2}^j$ are the coefficients to the B-spline expansion. Similarly $\|a_{1,1}^j - a_{1,2}^j\|_\infty^2 \leq \|\phi_{1,1}^j - \phi_{1,2}^j\|_\infty^2$, where $\phi_{1,1}^j$ and $\phi_{1,2}^j$ are the corresponding B-spline coefficients. Lastly, $\|F_{0,1} - F_{0,2}\|_\infty^2 \leq \|\kappa_{0,1} - \kappa_{0,2}\|_\infty^2$ with $\kappa_{0,1}$ and $\kappa_{0,2}$ as corresponding B-spline coefficients. We can show that

$$\begin{aligned} \frac{1}{n} \sum_{i=1}^n d_H^2(p_{i1}, p_{i2}) &\leq \frac{(\sigma_1 - \sigma_2)^2}{\sigma_1^2 + \sigma_2^2} + 2 \sum_j [\|\phi_{0,1}^j - \phi_{0,2}^j\|_\infty^2 + \|\phi_{1,1}^j - \phi_{1,2}^j\|_\infty^2 \\ &\quad + (\sum_k (\phi_{0,1k}^j)^2 + (\phi_{1,1k}^j)^2) D^2 (\|\beta_0 - \beta_1\|_2^2 \lambda_1 + \|\eta_0 - \eta_1\|_2^2 \lambda_2)] \\ &\quad + 2 \|\kappa_{0,1} - \kappa_{0,2}\|_\infty^2 (\max_j (a_{1,1}^j)^2) \end{aligned} \quad (6.1)$$

The proof of (6.1) is in the Section 10.

Lower bound for the Hellinger distance

By Lemma 2, we obtain that as $\sum_i d_H^2(p_{i1}, p_{i2}) \rightarrow 0$, $\sigma_1 \rightarrow \sigma_2$ and $\mu_{i1} \rightarrow \mu_{i2}$ for each i . As $F_{0,1}(0) = 0$ and $F_{0,2}(0) = 0$, we have $a_{0,1}^j(X'_i \beta_1, Z'_i \eta_1) \rightarrow a_{0,2}^j(X'_i \beta_2, Z'_i \eta_2)$. On the other hand $F_{0,1}(1) = 1$ and $F_{0,2}(1) = 1$ imply $a_{1,1}^j(X'_i \beta_1, Z'_i \eta_1) \rightarrow a_{1,2}^j(X'_i \beta_2, Z'_i \eta_2)$. This implies $F_{0,1} \rightarrow F_{0,2}$ pointwise at the given time points.

The following two inequalities can be used to get the lower bound in terms of difference of the functions :

$$\begin{aligned} (g + h)^2 + g^2 &= 0.5(0.5((2g + h)^2 + h^2) + (g + h)^2 + g^2) \\ &\geq 0.25h^2 + 0.5g^2 \end{aligned} \quad (6.2)$$

$$\begin{aligned} (g_1 h_1 - g_2 h_2)^2 + (g_1 - g_2)^2 &= (g_1(h_1 - h_2) + h_2(g_1 - g_2))^2 \\ &\quad + h_2^2(g_1 - g_2)^2 + (1 - h_2^2)(g_1 - g_2)^2 \\ &\geq g_1^2(h_1 - h_2)^2 + (g_1 - g_2)^2 \end{aligned} \quad (6.3)$$

On applying the two inequalities in (6.2) and (6.3) repeatedly, we get

$$\begin{aligned} \frac{1}{n} \sum_{i,j,t} (F_{\Theta_1}(i, j, t) - F_{\Theta_2}(i, j, t))^2 &\geq \bar{T} C_1 \sum_{i,j} (a_{0,1}^j(X'_i \beta_1, Z'_i \eta_1) - a_{0,2}^j(X'_i \beta_2, Z'_i \eta_2))^2 \\ &\quad + \bar{T} C_2 \sum_{i,j} (a_{1,1}^j(X'_i \beta_1, Z'_i \eta_1) - a_{1,2}^j(X'_i \beta_2, Z'_i \eta_2))^2 \\ &\quad + \frac{1}{n} \sum_i T_i \sum_{t=1}^{T_i} C_3 \min_j (a_{1,1}^j)^2 (F_{0,1}(t) - F_{0,2}(t))^2 \end{aligned}$$

for some positive constants C_1, C_2 and C_3 .

From the identifiability conditions on the single index model we conclude that as the functional values come close, the parameters and functions themselves become close as the number of observations goes to infinity. On the other hand $F_{0,1}(\cdot)$ approaches $F_{0,2}(\cdot)$ for all those points where there is an observation.

We make the further assumptions on the unknown functions:

- Assumption 1. The true functions are Lipschitz continuous.
- Assumption 2. There exists a large number $M > 0$, such that for all $j = 1, \dots, J$ the functions $a_{1,0}^j < M$.
- Assumption 3. There exists $L_1 > 0$, $L_2 > 0$ such that $|(a_{0,0}^j)'(\cdot)| < L_1$ and $|(a_{1,0}^j)'(\cdot)| < L_2$, where $(a_{0,0}^j)'(\cdot)$ and $(a_{1,0}^j)'(\cdot)$ denote the first derivatives of $a_{0,0}(\cdot)$ and $a_{1,0}(\cdot)$ respectively.

Let $\Theta_0 = (\beta_0, \eta_0, \sigma_0, a_{0,0}, a_{1,0}, F_{0,0})$ be the true set of parameters. For alternating Θ_1 , we get

$$\begin{aligned} & \frac{1}{n} \sum_{i,j,t} (F_{\Theta_0}(i, j, t) - F_{\Theta_1}(i, j, t))^2 \\ & \leq \bar{T} [2 \sum_j \|a_{0,0}^j - a_{0,1}^j\|_{\infty}^2 + 4J(L_1 + L_2)(\|\beta_0 - \beta_1\|_2^2 \lambda_1 + \|\eta_0 - \eta_1\|_2^2 \lambda_2) \\ & \quad + 2JM^2 \|F_{0,0} - F_{0,1}\|_{\infty}^2 + 2 \sum_j \|a_{1,0}^j - a_{1,1}^j\|_{\infty}^2] \end{aligned} \quad (6.4)$$

The proof of (6.4) is given in the Section 10.

Note the following relations

$$\begin{aligned} & \frac{1}{n} \sum_{i=1}^n (\mu_0^i - \mu_1^i)'(\mu_0^i - \mu_1^i) = \frac{1}{n} \sum_{i,j,t} (F_{\Theta_0}(i, j, t) - F_{\Theta_1}(i, j, t))^2, \\ & \frac{1}{n} \sum_{i=1}^n K(p_{i0}, p_{i1}) = J\bar{T} \log\left(\frac{\sigma_1}{\sigma_0}\right) - \frac{1}{2} \left[J\bar{T} - \frac{1}{n} \left(\sum_{i=1}^n \frac{(\mu_0^i - \mu_1^i)'(\mu_0^i - \mu_1^i)}{\sigma_1^2} \right) - J\bar{T} \frac{\sigma_0^2}{\sigma_1^2} \right]. \end{aligned}$$

Except for θ , all other components are fixed dimensional. Positive prior probability for those cases can easily be verified. Let s be a binary array of length $p - 1$ which has 1 at places where θ_i s are not equal to the null values. Null values are $\pi/2$ for initial $p - 2$ angles and 0 or $\pi/2$ for last angle. If θ_{p-1} is not among those s angles, it may be zero as well. Let s_0 denotes the true value of s . We can represent $\theta = \frac{\pi}{2}(1 - s) + s \cdot \theta$ if all the null values of θ are $\pi/2$ where $s \cdot \theta$ denotes element wise multiplication of s and θ . Thus we obtain using the fact that each polar angle is $\leq 2\pi$,

$$\|\theta_0 - \theta_1\|_2^2 \leq \left(\frac{\pi}{2}\right)^2 \|s_1 - s_0\|_2^2 + \|s_1 \cdot \theta_1 - s_0 \cdot \theta_0\|_2^2$$

$$\leq \left(\frac{\pi}{2}\right)^2 \|s_1 - s_0\|_2^2 + (2\pi)^2 \|s_0 - s_1\|_2^2 + \|s_0 \cdot \theta_1 - s_0 \cdot \theta_0\|_2^2. \quad (6.5)$$

Let for a given dimension D , B-spline basis functions be $\psi_{D,1}, \dots, \psi_{D,D} : X \rightarrow [0, 1]$ on a domain \mathcal{X} , a bounded convex set in \mathbb{R}^d . Let us define the matrix Φ of dimension $2J \times D^2$ of which the first J rows are $\{\phi_{0,0}^1, \dots, \phi_{0,0}^J\}$ and the last J rows are $\{\phi_{1,0}^1, \dots, \phi_{1,0}^J\}$.

Priors on each row of Φ and κ are multivariate normals and the supremum norm is used to induce a metric and $\Pi(D = j) = b_1 \exp(-b_2 j (\log j)^{b_3})$ where $0 \leq b_3 \leq 1$.

Lemma 3. *For large j , we can show $\exp(-b_2 j (\log j)^{b_3}) \asymp \Pi(D = j) \leq \Pi(D \geq j) \asymp \exp(-b_2 j (\log j)^{b_3})$*

Proof. The first relation trivially follows from the definition of $\Pi(D = j)$. For the other part we can show $\Pi(D = j + 1) = g(j)\Pi(D = j)$, where $g(j) = \exp(-b_2(j + 1)(\log(j + 1))^{b_3} + b_2 j (\log j)^{b_3})$. Now for large enough d we have $g(m + 1) < g(m) < 1$ for all $m > j$ and $g(\infty) = 0$.

$$\Pi(D \geq j) = \sum_{l=j}^{\infty} \Pi(D = l) \leq (1 - g(j))^{-1} \Pi(D = j)$$

For large j , thus we have $\Pi(D \geq j) \asymp \exp(-b_2 j (\log j)^{b_3})$. \square

For each row of Φ and κ , following assertions hold as we have multivariate normal prior on these vectors.

- (A1) $\Pi(\|\Phi_i - \Phi_i^0\| \leq \epsilon) \geq \exp(-t_2 D^2 \log_- \epsilon)$ for every $\Phi_i^0 \in \mathbb{R}^{D^2}$ with $\|\Phi_i^0\|_\infty \leq H$, for given positive constants t_2 and H , and every sufficiently small $\epsilon > 0$. Similarly $\Pi(\|\kappa - \kappa_0\| \leq \epsilon) \geq \exp(-t_1 D \log_- \epsilon)$; here $\log_- x = \max(\log(1/x), 0)$ i.e. the negative part of $\log x$.
- (A2) $\Pi(\Phi_i \notin [-M, M]^{D^2}) \leq D^2 e^{-cM^2}$, for every M . Similarly, $\Pi(\kappa \notin [-M, M]^D) \leq D e^{-cM^2}$ for some constant c .
- (A3) For the uniform norm, $\|a_{0,0}^j - a_{0,1}^j\|_\infty \leq D \|\phi_{0,0} - \phi_{0,1}\|_2$, $\|a_{1,0}^j - a_{1,1}^j\|_\infty \leq D \|\phi_{1,0} - \phi_{1,1}\|_2$ and $\|F_{0,0} - F_{0,1}\|_\infty \leq \sqrt{D} \|\kappa_0 - \kappa_{0,1}\|_2$.

We have total $2J + 1$ functions in the model. Let \mathcal{L}_0 be the list of true functions i.e. $\mathcal{L}_0 = \{a_{0,0}^j, a_{1,0}^j, F_0 : j = 1, \dots, J\}$. We need to modify the Lemma 10.20 from page 290 of [Ghosal and van der Vaart \(2017\)](#) for this case. Due to Lemma 3, and (A1), (A2) and (A3) the required support conditions on prior for Lemma 10.20 hold.

Let d be the metric on the above vector of functions such that $d(\mathcal{L}_0, (\Phi' \psi_{D^2}, \kappa' \psi_D)) = \max\{\|a_{0,0}^j - \Phi'_j \psi_{D^2}\|_\infty, \|a_{1,0}^j - \Phi'_{J+j} \psi_{D^2}\|_\infty, \|F_{0,0} - \kappa' \psi_D\|_\infty : 1 \leq j \leq J\}$.

To show posterior contraction, we construct a sieve for the parameter space. We consider the sieves of the form $\mathcal{W}_{D_n, M_n} = \{\Phi' \psi_{D^2}, \kappa' \psi_D : D \leq D_n, \|\phi_{0,i}^j\|_\infty \leq M_n, \|\kappa\|_\infty \leq M_n \text{ for } i = 0, 1; j \leq J\}$ and $\mathcal{H}_n = \{\varkappa = (\sigma, \alpha, s, \theta) : e^{n\bar{\epsilon}_n^2/t_6} \geq \sigma \geq n^{-1/t_5}\}$

Lemma 4. For a given vector of functions \mathcal{L}_0 , there exists a positive integer \bar{D}_n and $((\Phi_0))_i \in [-H, H]^{\bar{D}_n^2}$ for all $i = 1, \dots, J$ and $\kappa_0 \in [-H, H]^{\bar{D}_n}$ with $d(\mathcal{L}_0, (\Phi'_0 \psi_{\bar{D}_n^2}, \kappa'_0 \psi_{\bar{D}_n})) \leq \bar{\epsilon}_n$, such that for $\bar{\epsilon}_n/\bar{D}_n$ sufficiently small and $\epsilon_n \leq D_n^{3/2} M_n$, we have,

$$\Pi((\Phi' \psi_{D^2}, \kappa' \psi_D) : d(\mathcal{L}_0, (\Phi' \psi_{D^2}, \kappa' \psi_D)) \leq 2\bar{\epsilon}_n) \geq A(\bar{D}_n) \left(\frac{\bar{\epsilon}_n}{\bar{D}_n} \right)^{t_1 \bar{D}_n^2 J} \left(\frac{\bar{\epsilon}_n}{\sqrt{\bar{D}_n}} \right)^{t_2 \bar{D}_n},$$

$$\log \mathcal{N}(\epsilon_n, \mathcal{W}_{D_n, M_n}, d) \lesssim J D_n^2 \log(3D_n^3 M_n / \epsilon_n) + D_n \log(3D_n^{3/2} M_n / \epsilon_n),$$

$$\Pi(\mathcal{W}_{D_n, M_n}^c) \leq A(D_n) + (JD_n^2 + D_n) e^{-M_n^2},$$

where $A(j) = \exp(-b_2 j(\log j)^{b_3})$

Proof. The proof of the above Lemma is similar to that of Lemma 10.20 in [Ghosal and van der Vaart \(2017\)](#). Only for the first assertion we need to use the fact that our metric is a supremum norm over an array of functions. Using the results in (A1), (A2), (A3) and Lemma 3, we get the above forms. \square

Using Lemma 4, we can now modify Theorem 10.21 from page 291 of [Ghosal and van der Vaart \(2017\)](#) to get the contraction rates.

Theorem 5. Let $\epsilon_n \geq \bar{\epsilon}_n$ be sequences of positive numbers with $\epsilon_n \rightarrow 0$ and $n\bar{\epsilon}_n^2 \rightarrow \infty$, and let $D_n, \bar{D}_n \geq 3, M_n > 0$ be such that, for some sequence $b_n \rightarrow \infty$,

$$\inf_{\Phi, \kappa} d(\mathcal{L}_0, (\Phi' \psi_{\bar{D}_n^2}, \kappa' \psi_{\bar{D}_n})) \leq \bar{\epsilon}_n, \quad (6.6)$$

$$\bar{D}_n (\log \bar{D}_n)^{b_3 \vee 1} + \bar{D}_n^2 \log_- \bar{\epsilon}_n \lesssim n\bar{\epsilon}_n^2, \quad (6.7)$$

$$D_n^2 \log \left(\frac{D_n M_n n}{\epsilon_n} \right) \lesssim n\epsilon_n^2, \quad (6.8)$$

$$D_n (\log D_n)^{b_3} \geq b_n n \bar{\epsilon}_n^2, \quad (6.9)$$

$$\log D_n + b_n n \bar{\epsilon}_n^2 \leq M_n^2. \quad (6.10)$$

Let the prior on κ satisfy, for some \mathcal{H}_n ,

$$\Pi(\kappa : \|\kappa - \kappa_0\| < \bar{\epsilon}_n) \geq e^{-n\bar{\epsilon}_n^2}, \quad (6.11)$$

$$\log_+ \text{diam}(\mathcal{H}_n) \leq n\bar{\epsilon}_n^2, \quad (6.12)$$

$$\Pi(\kappa \notin \mathcal{H}_n) \leq e^{-b_n n \bar{\epsilon}_n^2} \quad (6.13)$$

Assume that the root averaged squared Hellinger distance (d_n) of $\Theta_1, \Theta_2 \in \mathcal{W}_{D_n, M_n} \times \mathcal{H}_n$ and for average Kullback-Leibler divergence of Θ_0, Θ_1 satisfy the conditions, for some $a, e > 0$

$$n^{-e} d_n(\Theta_1, \Theta_2) \lesssim d(\Theta_1, \Theta_2)^a + \|\kappa_1 - \kappa_2\|^a, \quad (6.14)$$

and for Θ_0 and Θ_1 sufficiently close,

$$\frac{1}{n} \sum_{i=1}^n K(p_{i0}, p_{i1}) \lesssim d^2(\Theta_0, \Theta_1) + \|\kappa_1 - \kappa_2\|^2. \quad (6.15)$$

Then $P_{\Theta_0}^n \Pi_n(d_n(\Theta, \Theta_0) > K_n \epsilon_n) \rightarrow 0$, for every $K_n \rightarrow \infty$, where $P_{\Theta_0}^n$ is the joint distribution of the vector of observations.

Proof of the above theorem can follow that of Theorem 10.21 in [Ghosal and van der Vaart \(2017\)](#). This Theorem extends the result of previous theorem of [Ghosal and van der Vaart \(2017\)](#) for an array of functions.

We just need to verify the above conditions and get the contraction rate.

For $\Theta_1, \Theta_2 \in \mathcal{W}_{D_n, M_n} \times \mathcal{H}_n$, using the result in (6.1) we get

$$\begin{aligned}
d_n &= \frac{1}{n} \sum_{i=1}^n d_H^2(p_{i1}, p_{i2}) \\
&\leq \frac{1}{2} n^{2/t_5} (\sigma_1 - \sigma_2)^2 + 2 \sum_j [\|\phi_{0,1}^j - \phi_{0,2}^j\|_\infty^2 + \|\phi_{1,1}^j - \phi_{1,2}^j\|_\infty^2] \\
&\quad + 8M_n^2 D_n^3 (\|\theta_1 - \theta_2\|_2^2 \lambda_1 + \|\alpha_1 - \alpha_2\|_2^2 \lambda_2) + 2D_n M_n^2 \|\kappa_{0,1} - \kappa_{0,2}\|_\infty^2 \\
&\leq \frac{1}{2} n^{2/t_5} (\sigma_1 - \sigma_2)^2 + 2 \sum_j [\|\phi_{0,1}^j - \phi_{0,2}^j\|_\infty^2 + \|\phi_{1,1}^j - \phi_{1,2}^j\|_\infty^2] \\
&\quad + 8M_n^2 D_n^3 \left(\left(\frac{17}{4} \pi^2 \|s_1 - s_2\|_2^2 + \|s_1 \cdot \theta_1 - s_1 \cdot \theta_2\|_2^2 \right) \lambda_1 + \|\alpha_1 - \alpha_2\|_2^2 \lambda_2 \right) \\
&\quad + 2D_n M_n^2 \|\kappa_{0,1} - \kappa_{0,2}\|_\infty^2
\end{aligned} \tag{6.16}$$

For $X \sim \text{Be}(M_1, M_2)$ with $M_1 < 1 \leq M_2$, using the transformation $y = x/(1 - \epsilon)$

$$\begin{aligned}
P(X > \epsilon) &= \frac{1}{B(M_1, M_2)} \int_\epsilon^1 x^{M_1-1} (1-x)^{M_2-1} dx \\
&= \frac{1}{B(M_1, M_2)} \int_0^{1-\epsilon} (1-x)^{M_1-1} x^{M_2-1} dx \\
&= \frac{(1-\epsilon)^{M_2}}{B(M_1, M_2)} \int_0^1 (1-(1-\epsilon)y)^{M_1-1} y^{M_2-1} dy, \\
&\leq (1-\epsilon)^{M_2}
\end{aligned} \tag{6.17}$$

The last inequality is due to $(1-(1-\epsilon)y)^{M_1-1} \leq (1-y)^{M_1-1}$ as $M_1 < 1$

We have

$$P(s_{1i} = 1) = \frac{\gamma}{\gamma + (1-\gamma) \frac{\Gamma(M_1+M_2)}{\Gamma(M_1)\Gamma(M_2)} (\theta'_i)^{M_1-1} (1-\theta'_i)^{M_2-1}},$$

here we define $\theta'_i = 1 - \frac{\min(\theta_i, \pi - \theta_i)}{\pi/2}$ for $1 \leq i \leq (p-2)$ and $\theta''_{p-1} = \frac{\theta_{p-1}}{\pi/2} - \mathbb{1}(\theta_{p-1} > \pi/2) - \mathbb{1}(\theta_{p-1} > \pi) - \mathbb{1}(\theta_{p-1} > 3\pi/2)$. Then we would reduce it further to $\theta'_{p-1} = \frac{4}{\pi} \min(\theta''_{p-1}, \pi/2 - \theta''_{p-1})$. This reparametrization is only required because the beta density is defined in $[0, 1]$.

We have i th polar angle in the model if and only if

$$\begin{aligned} P(s_{1i} = 1) &> 0.5 \\ \Leftrightarrow \frac{\gamma}{1-\gamma} &> \frac{\Gamma(M_1 + M_2)}{\Gamma(M_1)\Gamma(M_2)}(\theta'_i)^{M_1-1}(1-\theta'_i)^{M_2-1} \\ \Leftrightarrow \theta'_i &> \Psi\left(\frac{\gamma}{1-\gamma}\right) \end{aligned}$$

The last inequality is deduced from the fact that $M_1 < 1 \leq M_2$ and thus the beta density of θ'_i is decreasing in $[0, 1]$. Any upper bound on density will correspond to lower bound on the parameter θ'_i . We can also infer that Ψ will be a decreasing function in its argument. As M_2 increases in (6.17), $P(\theta'_i > \epsilon)$ decreases to zero for each ϵ and thus chances of ‘ $P(s_{1i} = 1) > 0.5$ ’ goes to zero for most of the i ’s for fixed γ . The prior would make most of the entries in s_1 and s_2 zero. To achieve $\|s_1 - s_2\|_2^2$ small, s_1 necessarily needs to coincide with s_2 . We note that $s_1 \cdot \theta_1 - s_1 \cdot \theta_2$ is in a low dimensional space due to the element wise multiplication of θ_1 and θ_2 with s_1 .

We need to vary M_2 with n . Thus we consider M_{2n} . From 6.17, we obtain $(1 - \epsilon_n)^{M_{2n}} = o(1/p)$ which implies $M_{2n} > \frac{\log p}{\epsilon_n}$.

Using the fact that $\log(1 + x) \leq |x|$, we obtain from 6.4 for Θ_0 and Θ_1 sufficiently close,

$$\begin{aligned} & \frac{1}{n} \sum_{i=1}^n K(p_{i0}, p_{i1}) \\ & \lesssim J\bar{T} \frac{|\sigma_0^2 - \sigma_1^2|}{\sigma_0^2} + \bar{T}[2 \sum_j (\|\phi_{0,0}^j - \phi_{0,1}^j\|_\infty^2 + \|\phi_{1,0}^j - \phi_{1,1}^j\|_\infty^2) \\ & \quad + 8J(L_1 + L_2)(\|\theta_0 - \theta_1\|_2^2 \lambda_1 + \|\alpha_0 - \alpha_1\|_2^2 \lambda_2) + 2JM^2 \|\kappa_{0,0} - \kappa_{0,1}\|_\infty^2] \\ & \lesssim J\bar{T} \frac{|\sigma_0^2 - \sigma_1^2|}{\sigma_0^2} + \bar{T}[2 \sum_j (\|\phi_{0,0}^j - \phi_{0,1}^j\|_\infty^2 + \|\phi_{1,0}^j - \phi_{1,1}^j\|_\infty^2) \\ & \quad + 8J(L_1 + L_2)((\frac{17}{4}\pi^2 \|s_1 - s_0\|_2^2 + \|s_0 \cdot \theta_1 - s_0 \cdot \theta_0\|_2^2)\lambda_1 + \|\alpha_0 - \alpha_1\|_2^2 \lambda_2) \\ & \quad + 2JM^2 \|\kappa_{0,0} - \kappa_{0,1}\|_\infty^2] \end{aligned} \tag{6.18}$$

Thus (6.14) and (6.15) from Theorem 5 are verified. Let ι be the regularity level of the true function in each direction. Then for B-spline approximation of the true functions w_{10} (univariate) and w_{20} (bivariate) with D number of basis functions in each direction we have $\inf_\zeta \|w_{10} - \zeta'_1 \psi_D\| \lesssim D^{-\iota}$ for univariate functions and $\inf_\zeta \|w_{20} - \zeta'_2 \psi_D\| \lesssim D^{-\iota}$ for bivariate functions. The conditions (6.7)–(6.10) change accordingly such that right hand side of the inequalities in Lemma 4 becomes of the order $n\epsilon_n^2$.

Theorem 6. *Under the assumed conditions on prior and true functions, the posterior contraction rate of the proposed double single index model is*

$$\max(n^{-\iota/(\iota+1)}(\log n)^{\iota/(\iota+1)\bar{b}_3 - b_3/2 + 1}, (n/\log^{\bar{b}_3/2} n)^{-\iota/(\iota+1)}),$$

where $\bar{b}_3 = b_3 \vee 1$

Proof. In our case $\inf_{\Phi, \kappa} d(\mathcal{L}_0, (\Phi' \psi_{\bar{D}_n^2}, \kappa' \psi_{\bar{D}_n})) \lesssim D_n^{-\iota}$. Combining with (6.8), we obtain that $\bar{D}_n^{-\iota} \lesssim \bar{\epsilon}_n$ and $\bar{D}_n^2 \log n \lesssim n \bar{\epsilon}_n^2$. Thus to satisfy (6.6)–(6.10) we choose $\bar{D}_n \asymp (n / \log^{\bar{b}_3/2} n)^{1/(\iota+1)}$, $\bar{\epsilon}_n \asymp (n / \log^{\bar{b}_3/2} n)^{-\iota/(\iota+1)}$, $\epsilon_n \gg n^{-\iota/(\iota+1)} (\log n)^{\iota/(\iota+1) \bar{b}_3 - \bar{b}_3/2 + 1}$ so that $D_n \gg n^{1/(\iota+1)} (\log n)^{(\iota/(\iota+1)) \bar{b}_3 - \bar{b}_3}$. Here the nuisance parameter set is κ . Conditions (6.11)–(6.13) for the prior on $\kappa = \sigma, \alpha, s, \theta$ of the Theorem 5 will automatically hold for above rates. We also need from 6.17 that $M_{2n} > \log p / [(n / \log^{\bar{b}_3/2} n)^{-\iota/(\iota+1)}]$ \square

7 Real data analysis

7.1 Modification of the model for real data application

Incorporating random effect and region wise varying effect

As the data is a longitudinal time series, it is reasonable to add subject specific random effect (τ_i) in the model and vary the effect of the low dimensional covariates region-wise. The new modified model will then become

$$\begin{aligned} Y_{ijt} &= F(i, j, t) + \tau_i + \epsilon_{ijt}, \epsilon_{ijt} \sim N(0, \sigma^2), \\ F(i, j, t) &= a_0^j(X_i' \beta, Z_i' \eta_j) - a_1^j(X_i' \beta, Z_i' \eta_j) F_0(t) \end{aligned} \quad (7.1)$$

We can take successive difference within a pair of individual, region over time and another successive differences within each individual over regions. These will not involve the random effect. Consistency of the posterior distribution given this reduced data will follow from the results we showed in Section 6. By plugging-in those estimates form the reduced model into the original model, we can consistently estimate random effects.

Prior on random effect

We put a Dirichlet process scale mixture of normal prior on the random effect.

Region wise varying effect with no SNP

To compare the results with Hostage et al. (2014), we also fit the following model without the SNPs,

$$\begin{aligned} Y_{ijt} &= F(i, j, t) + \tau_i + \epsilon_{ijt}, \epsilon_{ijt} \sim N(0, \sigma^2), \\ F(i, j, t) &= a_0^j(Z_i' \eta_j) - a_1^j(Z_i' \eta_j) F_0(t) \end{aligned} \quad (7.2)$$

Corresponding Linear Model

We compare the performance of our above non-linear models with following linear model,

$$\begin{aligned} Y_{ijt} &= H(i, j, t) + \tau_i + \epsilon_{ijt}, \epsilon_{ijt} \sim N(0, \sigma^2), \\ H(i, j, t) &= \varrho_{j0} + \varrho_{j,M}^0 Z_{i,M} + \varrho_{j,AD}^0 Z_{i,AD} + \varrho_{j,NC}^0 Z_{i,NC} + \varrho_{j,Allele4}^0 Z_{i,Allele4} \\ &\quad + \varrho_{j,Allele2}^0 Z_{i,Allele2} + \varrho_{j,Age}^0 Z_{i,Age} + \varrho_{j,AD,Allele2}^0 Z_{i,AD} Z_{i,Allele2} \end{aligned}$$

$$\begin{aligned}
& + \varrho_{j,AD,Allele4}^0 Z_{i,AD} Z_{i,Allele4} + \varrho_{j,NC,Allele2}^0 Z_{i,NC} Z_{i,Allele2} \\
& + \varrho_{j,NC,Allele4}^0 Z_{i,NC} Z_{i,Allele4} - [\varrho_{j1} + \varrho_{j,M}^1 Z_{i,M} + \varrho_{j,AD}^1 Z_{i,AD} + \varrho_{j,NC}^1 Z_{i,NC} \\
& + \varrho_{j,Allele4}^1 Z_{i,Allele4} + \varrho_{j,Allele2}^1 Z_{i,Allele2} + \varrho_{j,Age}^1 Z_{i,Age} \\
& + \varrho_{j,AD,Allele2}^1 Z_{i,AD} Z_{i,Allele2} + \varrho_{j,AD,Allele4}^1 Z_{i,AD} Z_{i,Allele4} \\
& + \varrho_{j,NC,Allele2}^1 Z_{i,NC} Z_{i,Allele2} + \varrho_{j,NC,Allele4}^1 Z_{i,NC} Z_{i,Allele4}] t
\end{aligned} \tag{7.3}$$

We have data for total thirteen brain regions along with whole brain over time for 748 individuals. For each individual, we have covariate information which are summarized in Table 3. The standard deviations for age in each groups are mentioned in bracket.

Table 3: Demographic table

	Female	Male
No cognitive impairment (NC)	99	114
Alzheimer's disease (AD)	84	94
Mild cognitive impairment (MCI)	122	235
APOEgene allele2	29	29
APOEgene allele4	150	223
Average age	73.51 (6.67)	74.60 (6.80)

We first fit the model in (7.2) and the following linear model in (7.3) in accordance with [Hostage et al. \(2014\)](#) and compare the prediction MSE as well as fitted relative MSE. Prediction error gives us predictive performance and fitted relative MSE helps to judge reliability of inference. We consider 17 basis B-spline functions for univariate and 17^2 basis functions for bivariate cases.

Linear model gives the prediction error 0.00123 whereas that in our non-linear model improves to 2.89107e-04. The model in (7.1) with SNPs betters the prediction error to 1.14504e-04. To calculate the region-wise effects of the low dimensional covariates on atrophy we further the estimated partial derivative with respect to time on the low dimensional covariates. We further compare the fit across the three models - linear, non linear without SNP, and non linear with SNP in Table 4 by means of relative fitted MSE based on the whole dataset. The formula for relative fitted MSE for a given region j is defines as $1 - R^2 = \frac{1}{n} \sum_i \frac{1}{T_i} \frac{\sum_{t=1}^{T_i} (Y_{ijt} - \hat{Y}_{ijt})^2}{\sum_{t=1}^{T_i} (Y_{ijt} - \bar{Y}_{ij})^2}$; here \hat{Y}_{ijt} represents fitted value of Y_{ijt} and \bar{Y}_{ij} mean over all the observations for i th individual and j th region. For prediction error, we divide the whole dataset into training and testing. We use stratified type sampling using each subject-region pair as strata so that training will have all the individuals that belong to testing set. This is important for prediction with a random effect in the model.

To obtain marginal effect of the covariate on atrophy we regress the estimated slope function on the covariates. Regression coefficient corresponding to a covariate is analogous to average partial derivative of the function with respect to the covariate. For

Table 4: Relative fitted MSE

Region name	Linear	Non-linear without SNP	Non-linear with SNP
Total Brain	0.01429	0.00033	0.00031
Ventricles	0.01066	0.00142	0.00142
Left Hippocampus	0.00653	0.00033	0.00033
Right Hippocampus	0.00661	0.00031	0.00031
Left inferior lateral ventricle	0.00507	0.00303	0.00303
Right inferior lateral ventricle	0.00526	0.00354	0.00354
Left Medial Temporal	0.53476	0.01827	0.01826
Right Medial Temporal	0.49215	0.01612	0.01610
Left Inferior Temporal	0.48042	0.01352	0.01351
Right Inferior Temporal	0.49338	0.01480	0.01480
Left Fusiform	0.63526	0.01661	0.01656
Right Fusiform	0.63618	0.01530	0.01529
Left Entorhin	0.32989	0.04184	0.04183
Right Entorhin	0.31116	0.04395	0.04390

binary covariate, the partial derivative with respect to Z_k is to be replaced by a difference to calculate an effect for region j :

$$\{(a_1^j(X_i'\beta, Z_i'\eta_j)|_{Z_{ik}=1, Z_{im}=0 \forall m \neq k} - a_1^j(X_i'\beta, Z_i'\eta_j)|_{Z_{im}=0, \forall m}) \frac{dF_0(t)}{dt}$$

And for interaction between Z_k and Z_l , the expression will become

$$\{(a_1^j(X_i'\beta, Z_i'\eta_j)|_{Z_{ik}=1, Z_l, Z_{im}=0 \forall m \neq k} - a_1^j(X_i'\beta, Z_i'\eta_j)|_{Z_{ik}=1, Z_{im}=0, \forall m} - a_1^j(X_i'\beta, Z_i'\eta_j)|_{Z_{il}=1, Z_{im}=0, \forall m} + a_1^j(X_i'\beta, Z_i'\eta_j)|_{Z_{im}=0, \forall m}) \frac{dF_0(t)}{dt}$$

For continuous covariate we regress the partial derivative on the covariate to get marginal main effect. Estimated parameters related to atrophy are given below in Table 6 for non-linear model and in Table 7 for the linear model corresponding to whole brain. Here positive values mean atrophy.

We map the significant SNPs from our analysis to corresponding gene ids using the R packages **biomaRt** and **rsnps**. We get following genes SLC6A1, LRBA, KCNIP4, ADGRL3, SORBS2, MND1, LPAR3, SHROOM3, SORCS3, NPY2R and CWF19L2. Their average effects on atrophy are also estimated and it is recorded in Table 5.

8 Conclusions and discussion

We fit a bivariate single index model to capture the volumetric change of different cortical regions in the human brain. There are both high and low-dimensional covariates as input to the unknown functions determining initial configuration and rate of change of different regions. To tackle the high dimensional covariate within a single index model, we provide a new technique to assign sparse prior in this paper. Posterior consistency results are also established. An ‘R’ package is attached with this paper as a supplementary material. This can be used to fit high and low dimensional single index models. This package can fit a single index model with only one input or two inputs with at

Table 5: SNPs selected after variable selection from non-linear model along with gene names and main effect on slope

	SNP name	Gene name	Overall
			Main Effect
1	rs9990174	SLC6A1	0.00172
2	rs999784	LRBA	0.00222
3	rs9998327	KCNIP4	0.00011
4	rs9998456	ADGRL3	0.00029
5	rs9998709	SORBS2	0.00217
6	rs9999069	MND1	0.00022
7	rs999915	LPAR3	0.00017
8	rs9999448	SHROOM3	0.00399
9	rs999981	SORCS3	0.00347
10	rs9999820	NPY2R	0.00076
11	rs999985	CWF19L2	0.00157

Table 6: Estimates of covariates for Total Brain for slope from non-linear model

	Estimate	Std. Error	t value	p-value
time	0.0085	0.0006	13.2069	0.0000
APOEallele4:time	0.0080	0.0009	8.5275	0.0000
APOEallele2:time	0.0008	0.0013	0.6491	0.5163
Gender:time	0.0012	0.0005	2.2546	0.0242
MCI:time	-0.0045	0.0008	-5.8255	0.0000
AD:time	0.0081	0.0011	7.3063	0.0000
Age:time	0.0004	0.0003	1.4899	0.1364
APOEallele4:MCI:time	0.0043	0.0011	3.9985	0.0001
APOEallele4:AD:time	0.0072	0.0012	5.7506	0.0000
APOEallele2:MCI:time	0.0025	0.0020	1.2259	0.2204
APOEallele2:AD:time	-0.0001	0.0032	-0.0375	0.9701

Table 7: Estimates of covariates for Total Brain for slope from linear model

	Value	Std.Error	DF	t-value	p-value
time	0.013	0.001	2155	13.208	0.000
APOEallele4:time	0.000	0.001	2155	0.047	0.962
APOEallele2:time	-0.001	0.002	2155	-0.249	0.804
Gender:time	0.003	0.001	2155	3.077	0.002
MCI:time	0.006	0.001	2155	4.811	0.000
AD:time	0.014	0.002	2155	6.969	0.000
Age:time	-0.002	0.000	2155	-4.663	0.000
APOEallele4:MCI:time	0.004	0.002	2155	2.689	0.007
APOEallele4:AD:time	0.004	0.002	2155	2.105	0.035
APOEallele2:MCI:time	0.001	0.003	2155	0.292	0.770
APOEallele2:AD:time	-0.003	0.006	2155	-0.530	0.596

most one in shrinkage consideration. The function `betaupdate` of this package is used to generate MCMC samples for polar angles of β and η of our model.

In our results on the real dataset, we find allele 4 of APOE gene, Alzheimer's disease state, and their interaction as significant covariates for almost all the cases. The fact that allele 4 of APOE gene is significant was established in [Hostage et al. \(2014\)](#). They used linear model, similar to the model in (7.3). But in our estimates of parameters for linear case in Table 7, APOE allele 4 is not significant. Such is the case for several other regions in linear case. But in our non-linear setup it is significant for whole brain as well as for all other important regions as given in the region wise tables in Section 10. For some cases few of other covariates are also significant like mild cognitive impairment (MCI) disease state, and gender. The effect size of covariates on the the slope function and the derivative of time of the our model in 7.1 are similar. We get some other significant genes which are mentioned in Table 5. We observe that main effect of APOE allele 4 is more than each of the main effects of these other genes. Except for MND1 and LRBA, rest of the significant genes were found to be associated with the Alzheimer's Disease before. These genes are mentioned in following two websites which contains all the known genes associated with AD, http://amp.pharm.mssm.edu/Harmonizome/gene_set/alzheimer+disease/GWASdb+SNP-Phenotype+Associations and http://amp.pharm.mssm.edu/Harmonizome/gene_set/alzheimer%27s+disease/GAD+Gene-Disease+Associations. Thus these gene have shown significant effect of brain activity. Now, we get these genes significant in our atrophy study.

9 Acknowledgments

Data collection and sharing for this project was funded by the Alzheimer's's Disease Neuroimaging Initiative (ADNI) (National Institutes of Health Grant U01 AG024904) and DOD ADNI (Department of Defense award number W81XWH-12-2-0012). ADNI is funded by the National Institute on Aging, the National Institute of Biomedical Imaging and Bioengineering, and through generous contributions from the following: AbbVie, Alzheimer's Association; Alzheimer's Drug Discovery Foundation; Araclon Biotech; BioClinica, Inc.; Biogen; Bristol-Myers Squibb Company; CereSpir, Inc.; Cogstate; Eisai Inc.; Elan Pharmaceuticals, Inc.; Eli Lilly and Company; EuroImmun; F. Hoffmann-La Roche Ltd and its affiliated company Genentech, Inc.; Fujirebio; GE Healthcare; IXICO Ltd.; Janssen Alzheimer's Immunotherapy Research & Development, LLC.; Johnson & Johnson Pharmaceutical Research & Development LLC.; Lumosity; Lundbeck; Merck & Co., Inc.; Meso Scale Diagnostics, LLC.; NeuroRx Research; Neurotrack Technologies; Novartis Pharmaceuticals Corporation; Pfizer Inc.; Piramal Imaging; Servier; Takeda Pharmaceutical Company; and Transition Therapeutics. The Canadian Institutes of Health Research is providing funds to support ADNI clinical sites in Canada. Private sector contributions are facilitated by the Foundation for the National Institutes of Health (www.fnih.org). The grantee organization is the Northern California Institute for Research and Education, and the study is coordinated by the Alzheimer's's Therapeutic Research Institute at the University of Southern California. ADNI data are disseminated by the Laboratory for Neuro Imaging at the University of Southern California.

The first author would like to thank Mr. Kushal Kumar Dey for helping him how to build an ‘R’ package.

10 Appendix

Lemma 1

Proof. Let $J_{\beta,\theta}$ be the Jacobian matrix for transformation from β to θ . Then from multivariate mean value theorem in (Burke (2014)), we have $\|\beta_1 - \beta_2\|_2 \leq \sup_{\beta,\theta} \|J_{\beta,\theta}\|_{\text{sp}} \|\theta_1 - \theta_2\|_2$, where $\|\cdot\|_{\text{sp}}$ denotes spectral norm of a matrix. Let us write $J_{\beta,\theta} = JL_{\beta,\theta} + JC$, where $JL_{\beta,\theta}$ corresponds to the lower triangular part of $J_{\beta,\theta}$ and $JC_{\beta,\theta}$ is matrix with only one band of elements above the diagonal. Then we can write

$$\|J_{\beta,\theta}\|_{\text{sp}} = \sup_{\|x\| \leq 1} \|J_{\beta,\theta}x\| \leq \sup_{\|x\| \leq 1} (\|JL_{\beta,\theta}x\| + \|JC_{\beta,\theta}x\|) \leq 1 + 1 = 2$$

because $JL_{\beta,\theta}$ is lower triangular with maximum diagonal entry one and the maximum element of $JC_{\beta,\theta}$ is also one. \square

Lemma 2

Proof. For $m_1 = 2\sigma_1\sigma_2/(\sigma_1^2 + \sigma_2^2)$ and $m_2 = (\mu_1 - \mu_2)'(\mu_1 - \mu_2)/(4(\sigma_1^2 + \sigma_2^2))$, $d_H^2(P, Q) = 1 - m_1^{k/2} \exp(-m_2)$. Note that $(1-x) \leq \exp(-x)$ for all real x and $\exp(-x) \leq (1-x/2)$ for positive $x \leq 1$. Also for $t \geq 2$, $(1-m_1^t) = 1 - ((m_1-1)+1)^t \leq C_1(1-m_1)$ as $0 \leq m_1 \leq 1$, where C_1 can be taken as the sum of the coefficients of the expansion $((m_1-1)+1)^t$. \square

To obtain (6.1), we can show following inequalities which will imply the result trivially.

$$\begin{aligned} & \sum_{i,j,t} (F_{\Theta_1}(i, j, t) - F_{\Theta_2}(i, j, t))^2 \\ & \leq 2 \sum_{i,j,t} [(a_{0,1}^j(X'_i \beta_1, Z'_i \eta_1) - a_{0,2}^j(X'_i \beta_2, Z'_i \eta_2))^2 + (a_{1,1}^j(X'_i \beta_1, Z'_i \eta_1)F_{0,1}(t) \\ & \quad - a_{1,2}^j(X'_i \beta_2, Z'_i \eta_2)F_{0,2}(t))^2], \end{aligned} \tag{10.1}$$

$$\begin{aligned} & (a_{0,1}^j(X'_i \beta_1, Z'_i \eta_1) - a_{0,2}^j(X'_i \beta_2, Z'_i \eta_2))^2 \\ & = (a_{0,1}^j(X'_i \beta_1, Z'_i \eta_1) - a_{0,1}^j(X'_i \beta_2, Z'_i \eta_2) + a_{0,1}^j(X'_i \beta_2, Z'_i \eta_2) - a_{0,2}^j(X'_i \beta_2, Z'_i \eta_2))^2 \\ & \leq 2\|a_{0,1}^j - a_{0,2}^j\|_{\infty}^2 + 2(a_{0,1}^j(X'_i \beta_1, Z'_i \eta_1) - a_{0,1}^j(X'_i \beta_2, Z'_i \eta_2))^2, \end{aligned} \tag{10.2}$$

$$\begin{aligned} & \frac{1}{n} \sum_{i=1}^n (a_{0,1}^j(X'_i \beta_1, Z'_i \eta_1) - a_{0,1}^j(X'_i \beta_2, Z'_i \eta_2))^2 \\ & \leq \sum_k (\phi_{0,1k}^j)^2 D^2(\|\beta_0 - \beta_1\|_2^2 \lambda_1 + \|\eta_0 - \eta_1\|_2^2 \lambda_2), \end{aligned} \tag{10.3}$$

$$\begin{aligned}
& \frac{1}{n} \sum_{i=1}^n (a_{1,1}^j(X'_i \beta_1, Z'_i \eta_1) - a_{1,1}^j(X'_i \beta_2, Z'_i \eta_2))^2 \\
& \leq \sum_k (\phi_{1,1k}^j)^2 D^2 (\|\beta_0 - \beta_1\|_2^2 \lambda_1 + \|\eta_0 - \eta_1\|_2^2 \lambda_2), \tag{10.4}
\end{aligned}$$

$$\begin{aligned}
& (a_{1,1}^j(X'_i \beta_1, Z'_i \eta_1) F_{0,1}(t) - a_{1,2}^j(X'_i \beta_2, Z'_i \eta_2) F_{0,2}(t))^2 \\
& \leq (a_{1,1}^j(X'_i \beta_2, Z'_i \eta_2))^2 (F_{0,1}(t) - F_{0,2}(t))^2 + (a_{1,1}^j(X'_i \beta_1, Z'_i \eta_1) \\
& - a_{1,2}^j(X'_i \beta_2, Z'_i \eta_2))^2 F_{0,2}(t)^2 \\
& \leq (a_{1,1}^j(X'_i \beta_1, Z'_i \eta_1) - a_{1,2}^j(X'_i \beta_2, Z'_i \eta_2))^2 \\
& + (F_{0,1}(t) - F_{0,2}(t))^2 \max_j (a_{1,1}^j(X'_i \beta_2, Z'_i \eta_2))^2; \tag{10.5}
\end{aligned}$$

above we have used $n^{-1} z' \sum_{i=1}^n X_i X'_i z \leq \lambda_1 z' z$, where λ_1 is the maximum eigenvalue of $n^{-1} \sum_{i=1}^n X_i X'_i$ and $z' n^{-1} \sum_{i=1}^n Z_i Z'_i z \leq \lambda_2 z' z$, where λ_2 is the maximum eigenvalue of $n^{-1} \sum_{i=1}^n Z_i Z'_i$.

To proof (6.4)

For Θ_0 using Lipschitz condition followed by the bound $z' n^{-1} \sum_{i=1}^n X_i X'_i z \leq \lambda_1 z' z$, where λ_1 is the maximum eigenvalue of $n^{-1} \sum_{i=1}^n X_i X'_i$ and $z' n^{-1} \sum_{i=1}^n Z_i Z'_i z \leq \lambda_2 z' z$, where λ_2 is the maximum eigenvalue of $n^{-1} \sum_{i=1}^n Z_i Z'_i$ gives

$$\begin{aligned}
& \frac{1}{n} \sum_{i=1}^n (a_{0,0}^j(X'_i \beta_0, Z'_i \eta_0) - a_{0,1}^j(X'_i \beta_1, Z'_i \eta_1))^2 \\
& \leq 2 \|a_{0,0}^j - a_{0,1}^j\|_\infty^2 + 2 \frac{1}{n} \sum_{i=1}^n (a_{0,0}^j(X'_i \beta_0, Z'_i \eta_0) - a_{0,0}^j(X'_i \beta_1, Z'_i \eta_1))^2 \\
& \leq 2 \|a_{0,0}^j - a_{0,1}^j\|_\infty^2 + 2L_1 \|\beta_0 - \beta_1\|_2^2 \lambda_1 + 2L_1 \|\eta_0 - \eta_1\|_2^2 \lambda_2
\end{aligned}$$

and,

$$\begin{aligned}
& \frac{1}{n} \sum_{i=1}^n (a_{1,0}^j(X'_i \beta_0, Z'_i \eta_0) F_{0,0}(t) - a_{1,1}^j(X'_i \beta_1, Z'_i \eta_1) F_{0,1}(t))^2 \\
& \leq M^2 \|F_{0,0} - F_{0,1}\|_\infty^2 + \frac{1}{n} \sum_{i=1}^n (a_{1,0}^j(X'_i \beta_0, Z'_i \eta_0) - a_{1,1}^j(X'_i \beta_1, Z'_i \eta_1))^2 \\
& \leq 2M^2 \|F_{0,0} - F_{0,1}\|_\infty^2 + 2 \|a_{1,0}^j - a_{1,1}^j\|_\infty^2 + 2L_2 \|\beta_0 - \beta_1\|_2^2 \lambda_1 + 2L_2 \|\eta_0 - \eta_1\|_2^2 \lambda_2
\end{aligned}$$

Thus using above two relations, we obtain (6.4)

Rest of the estimated tables

References

Ahveninen, J., Jääskeläinen, I. P., Belliveau, J. W., Hämäläinen, M., Lin, F., and Raij, T. (2012). "Dissociable Influences of Auditory Object vs. Spatial Attention on Visual

Table 8: Estimates for Ventricles for slope

	Estimate	Std. Error	t value	p-value
time	-0.0531	0.0043	-12.4436	0.0000
APOEallele4:time	0.0346	0.0062	5.5875	0.0000
APOEallele2:time	0.0646	0.0083	7.7687	0.0000
Gender:time	0.0108	0.0035	3.1423	0.0017
MCI:time	0.0133	0.0051	2.5784	0.0100
AD:time	0.0380	0.0074	5.1490	0.0000
Age:time	0.0004	0.0017	0.2557	0.7982
APOEallele4:MCI:time	-0.0199	0.0070	-2.8182	0.0049
APOEallele4:AD:time	-0.0292	0.0083	-3.5336	0.0004
APOEallele2:MCI:time	-0.0285	0.0133	-2.1435	0.0322
APOEallele2:AD:time	-0.0648	0.0210	-3.0828	0.0021

Table 9: Estimates for Left Hippocampus for slope

	Estimate	Std. Error	t value	p-value
time	0.0053	0.0011	4.8678	0.0000
APOEallele4:time	0.0094	0.0016	5.9956	0.0000
APOEallele2:time	0.0031	0.0021	1.4513	0.1468
Gender:time	-0.0023	0.0009	-2.6260	0.0087
MCI:time	0.0073	0.0013	5.6415	0.0000
AD:time	0.0038	0.0019	2.0409	0.0413
Age:time	0.0003	0.0004	0.6419	0.5210
APOEallele4:MCI:time	0.0003	0.0018	0.1548	0.8770
APOEallele4:AD:time	0.0076	0.0021	3.6578	0.0003
APOEallele2:MCI:time	-0.0099	0.0034	-2.9336	0.0034
APOEallele2:AD:time	-0.0017	0.0053	-0.3210	0.7482

System Oscillatory Activity.” *Public Library of Science One.* [2](#)

Alquier, P. and Biau, G. (2013). “Sparse Single-Index Model.” *Journal of Machine Learning Research*, 14: 243–280. [3](#)

Antoniadis, A., Grégoire, G., and McKeague, I. W. (2004). “Bayesian Estimation In Single-Index Models.” *Statistica Sinica*, 14: 1147–1164. [3](#)

Burke, J. V. (2014). “<https://sites.math.washington.edu/~burke/crs/408/lectures/L3-Multivariable-Calc-Review.pdf>.” [24](#)

Das, P. and Ghosal, S. (2017). “Bayesian quantile regression using random B-spline series prior.” *Computational Statistics and Data Analysis*, 109: 121–143. [6](#)

Fan, J. and Li, R. (2001). “Variable Selection via Nonconcave Penalized Likelihood and its Oracle Properties.” *Journal of the American Statistical Association*, 96(1). [11](#)

Ghosal, S. and van der Vaart, A. (2017). *Fundamentals of Nonparametric Bayesian Inference*. Cambridge University Press, Cambridge. [15](#), [16](#), [17](#)

Table 10: Estimates for Right Hippocampus for slope

	Estimate	Std. Error	t value	p-value
time	0.0044	0.0014	3.0999	0.0020
APOEallele4:time	0.0068	0.0021	3.3176	0.0009
APOEallele2:time	-0.0005	0.0028	-0.1961	0.8446
Gender:time	-0.0021	0.0011	-1.8073	0.0708
MCI:time	0.0121	0.0017	7.0573	0.0000
AD:time	0.0039	0.0025	1.5869	0.1126
Age:time	0.0006	0.0006	1.0891	0.2762
APOEallele4:MCI:time	0.0050	0.0023	2.1432	0.0322
APOEallele4:AD:time	0.0062	0.0027	2.2402	0.0252
APOEallele2:MCI:time	-0.0190	0.0044	-4.3067	0.0000
APOEallele2:AD:time	-0.0014	0.0070	-0.2000	0.8415

Table 11: Estimates for Left inferior lateral ventricle for slope

	Estimate	Std. Error	t value	p-value
time	-0.0628	0.0050	-12.4490	0.0000
APOEallele4:time	0.0458	0.0073	6.2527	0.0000
APOEallele2:time	0.0663	0.0098	6.7491	0.0000
Gender	0.0064:time	0.0041	1.5800	0.1142
MCI:time	0.0070	0.0061	1.1562	0.2477
AD:time	0.0472	0.0087	5.4115	0.0000
Age:time	-0.0011	0.0021	-0.5146	0.6068
APOEallele4:MCI:time	-0.0263	0.0083	-3.1526	0.0016
APOEallele4:AD:time	-0.0406	0.0098	-4.1578	0.0000
APOEallele2:MCI:time	-0.0329	0.0157	-2.0900	0.0367
APOEallele2:AD:time	-0.0716	0.0249	-2.8801	0.0040

Hostage, C. A., Choudhury, K. R., P.M., D., and J.R., P. (2014). “Mapping the Effect of the Apolipoprotein E Genotype on 4-Year Atrophy Rates in an Alzheimer Disease-related Brain Network.” *Radiology*, 271(1). [2](#), [19](#), [20](#), [23](#)

Jones, G. L. (2008). “<http://users.stat.umn.edu/~galin/icsprar.pdf>.”

Luo, S. and Ghosal, S. (2016). “Forward Selection and Estimation in High Dimensional Single Index Models.” *Stat Methodology*, 33: 172–179. [3](#)

Peng, H. and Huang, T. (2011). “Penalized least squares for single index models.” *J. Statist. Plann. Inference*, 141: 1362–1379. [3](#)

Petrella, J. (2013). “Neuroimaging and the search for a cure for Alzheimer disease.” *Radiology*, 269: 671–691. [1](#)

Radchenko, P. (2015). “High dimensional single index models.” *Journal of Multivariate Analysis*, 139: 266–282. [3](#)

Roy, A., Ghosal, S., Prescott, J., and Choudhury, K. (2017). “Bayesian Modeling of the Structural Connectome for Studying Alzheimer Disease.” *arXiv*, 1710.04560. [8](#)

Table 12: Estimates for Right inferior lateral ventricle for slope

	Estimate	Std. Error	t value	p-value
time	-0.0582	0.0055	-10.5815	0.0000
APOEallele4:time	0.0522	0.0080	6.5322	0.0000
APOEallele2:time	0.0567	0.0107	5.2879	0.0000
Gender:time	0.0117	0.0044	2.6227	0.0088
MCI:time	-0.0068	0.0066	-1.0216	0.3071
AD:time	0.0377	0.0095	3.9698	0.0001
Age:time	-0.0016	0.0022	-0.6927	0.4885
APOEallele4:MCI:time	-0.0253	0.0091	-2.7849	0.0054
APOEallele4:AD:time	-0.0445	0.0106	-4.1760	0.0000
APOEallele2:MCI:time	-0.0108	0.0171	-0.6293	0.5292
APOEallele2:AD:time	-0.0609	0.0271	-2.2470	0.0247

Table 13: Estimates for Left Medial Temporal for slope

	Estimate	Std. Error	t value	p-value
time	0.0042	0.0009	4.5576	0.0000
APOEallele4:time	0.0049	0.0013	3.6554	0.0003
APOEallele2:time	0.0032	0.0018	1.7819	0.0749
Gender:time	0.0012	0.0007	1.5881	0.1124
MCI:time	0.0061	0.0011	5.4561	0.0000
AD:time	0.0044	0.0016	2.7614	0.0058
Age:time	0.0001	0.0004	0.1820	0.8556
APOEallele4:MCI:time	0.0000	0.0015	0.0070	0.9944
APOEallele4:AD:time	0.0048	0.0018	2.6679	0.0077
APOEallele2:MCI:time	-0.0021	0.0029	-0.7264	0.4677
APOEallele2:AD:time	-0.0004	0.0045	-0.0802	0.9361

Thompson, P., Hayashi, K., and deZubicaray G. (2003). “Dynamics of gray matter loss in Alzheimer’s disease.” *Journal of Neuroscience*, 23: 994–1005. [2](#)

Tibshirani, R. (1996). “Regression Shrinkage and Selection via the Lasso.” *Journal of the Royal Statistical Society B*, 58: 267–288. [11](#)

Wang, H. (2009). “Bayesian estimation and variable selection for single index models.” *Computational Statistics and Data Analysis*, 53: 2617–2627. [3](#)

Wang, T., Xu, P., and Zhu, L. (2012). “Non-convex penalized estimation in high-dimensional models with single-index structure.” *The Journal of Multivariate Analysis*, 109: 221–235. [3](#)

Yu, Y. and Ruppert, D. (2002). “Penalized spline estimation for partially linear single index models.” *J. Amer. Statist. Assoc.*, 97: 1042–1054. [3](#)

Zhu, L. and Zhu, L. (2009). “Nonconcave penalized inverse regression in single-index models with high dimensional predictors.” *The Journal of Multivariate Analysis*, 100(5): 862–875. [3](#)

Table 14: Estimates for Right Medial Temporal for slope

	Estimate	Std. Error	t value	p-value
time	0.0083	0.0011	7.8945	0.0000
APOEallele4:time	0.0055	0.0015	3.6024	0.0003
APOEallele2:time	0.0010	0.0021	0.4745	0.6352
Gender:time	0.0009	0.0009	1.1006	0.2711
MCI:time	0.0022	0.0013	1.7644	0.0778
AD:time	0.0076	0.0018	4.1755	0.0000
Age:time	0.0001	0.0004	0.3162	0.7519
APOEallele4:MCI:time	0.0033	0.0017	1.9000	0.0575
APOEallele4:AD:time	0.0059	0.0020	2.9146	0.0036
APOEallele2:MCI:time	-0.0019	0.0033	-0.5662	0.5713
APOEallele2:AD:time	0.0001	0.0052	0.0202	0.9839

Table 15: Estimates for Left Inferior Temporal for slope

	Estimate	Std. Error	t value	p-value
time	0.0119	0.0012	10.0557	0.0000
APOEallele4:time	0.0148	0.0017	8.5908	0.0000
APOEallele2:time	-0.0045	0.0023	-1.9366	0.0529
Gender:time	0.0027	0.0010	2.7795	0.0055
MCI:time	0.0001	0.0014	0.0979	0.9220
AD:time	0.0100	0.0020	4.8879	0.0000
Age:time	0.0002	0.0005	0.4278	0.6689
APOEallele4:MCI:time	0.0101	0.0020	5.1644	0.0000
APOEallele4:AD:time	0.0134	0.0023	5.8357	0.0000
APOEallele2:MCI:time	0.0047	0.0037	1.2836	0.1994
APOEallele2:AD:time	0.0045	0.0058	0.7787	0.4362

Table 16: Estimates for Right Inferior Temporal for slope

	Estimate	Std. Error	t value	p-value
time	0.0128	0.0012	10.2825	0.0000
APOEallele4:time	0.0058	0.0018	3.2307	0.0012
APOEallele2:time	-0.0069	0.0024	-2.8457	0.0045
Gender:time	-0.0000	0.0010	-0.0120	0.9904
MCI:time	0.0017	0.0015	1.1410	0.2540
AD:time	0.0097	0.0022	4.5023	0.0000
Age:time	0.0003	0.0005	0.5489	0.5831
APOEallele4:MCI:time	0.0005	0.0021	0.2607	0.7943
APOEallele4:AD:time	0.0050	0.0024	2.0884	0.0368
APOEallele2:MCI:time	0.0024	0.0039	0.6120	0.5406
APOEallele2:AD:time	0.0084	0.0061	1.3714	0.1703

Table 17: Estimates for Left Fusiform for slope

	Estimate	Std. Error	t value	p-value
time	0.0125	0.0012	10.8219	0.0000
APOEallele4:time	0.0099	0.0017	5.8934	0.0000
APOEallele2:time	-0.0037	0.0022	-1.6363	0.1019
Gender:time	0.0025	0.0009	2.7219	0.0065
MCI:time	-0.0006	0.0014	-0.4046	0.6858
AD:time	0.0102	0.0020	5.1188	0.0000
Age:time	0.0001	0.0005	0.1823	0.8554
APOEallele4:MCI:time	0.0045	0.0019	2.3821	0.0173
APOEallele4:AD:time	0.0086	0.0022	3.8403	0.0001
APOEallele2:MCI:time	0.0049	0.0036	1.3715	0.1703
APOEallele2:AD:time	0.0053	0.0057	0.9349	0.3499

Table 18: Estimates for Right Fusiform for slope

	Estimate	Std. Error	t value	p-value
time	0.0070	0.0009	7.9958	0.0000
APOEallele4:time	0.0040	0.0013	3.1873	0.0015
APOEallele2:time	0.0002	0.0017	0.1286	0.8977
Gender:time	-0.0003	0.0007	-0.3875	0.6984
MCI:time	0.0028	0.0011	2.7002	0.0070
AD:time	0.0058	0.0015	3.8476	0.0001
Age:time	0.0003	0.0004	0.8653	0.3869
APOEallele4:MCI:time	-0.0004	0.0014	-0.2745	0.7837
APOEallele4:AD:time	0.0041	0.0017	2.4033	0.0163
APOEallele2:MCI:time	-0.0029	0.0027	-1.0650	0.2870
APOEallele2:AD:time	0.0005	0.0043	0.1248	0.9007

Table 19: Estimates for Left Entorhin for slope

	Estimate	Std. Error	t value	p-value
time	0.0003	0.0010	0.3323	0.7397
APOEallele4:time	0.0114	0.0014	7.9188	0.0000
APOEallele2:time	0.0031	0.0019	1.6251	0.1043
Gender:time	0.0053	0.0008	6.6727	0.0000
MCI:time	0.0054	0.0012	4.5014	0.0000
AD:time	0.0037	0.0017	2.1663	0.0304
Age:time	-0.0004	0.0004	-0.9482	0.3431
APOEallele4:MCI:time	0.0058	0.0016	3.5491	0.0004
APOEallele4:AD:time	0.0108	0.0019	5.6590	0.0000
APOEallele2:MCI:time	-0.0028	0.0031	-0.9120	0.3618
APOEallele2:AD:time	-0.0030	0.0049	-0.6087	0.5428

Table 20: Estimates for Right Entorhin for slope

	Estimate	Std. Error	t value	p-value
time	0.0068	0.0014	4.7268	0.0000
APOEallele4:time	0.0107	0.0021	5.1571	0.0000
APOEallele2:time	0.0050	0.0028	1.7943	0.0729
Gender:time	0.0042	0.0012	3.6146	0.0003
MCI:time	0.0167	0.0017	9.6401	0.0000
AD:time	0.0030	0.0025	1.2302	0.2187
Age:time	0.0002	0.0006	0.2899	0.7719
APOEallele4:MCI:time	0.0015	0.0024	0.6315	0.5278
APOEallele4:AD:time	0.0090	0.0028	3.2332	0.0012
APOEallele2:MCI:time	-0.0145	0.0045	-3.2515	0.0012
APOEallele2:AD:time	-0.0044	0.0071	-0.6283	0.5298